

## Review

# The Role of Nano-Sensors in Breath Analysis for Early and Non-Invasive Disease Diagnosis

Nefeli Lagopati <sup>1,2,\*</sup>, Theodoros-Filippos Valamvanos <sup>1,3,†</sup>, Vaia Proutsou <sup>1,3,†</sup>, Konstantinos Karachalios <sup>1,3,†</sup>, Natassa Pippa <sup>4</sup>, Maria-Anna Gatou <sup>5</sup>, Ioanna-Aglaia Vagena <sup>1</sup>, Smaragda Cela <sup>1,3</sup>, Evangelia A. Pavlatou <sup>5</sup>, Maria Gazouli <sup>1,6</sup> and Efstathios Efstathopoulos <sup>2,6</sup>

<sup>1</sup> Laboratory of Biology, Department of Basic Medical Sciences, Medical School, National and Kapodistrian University of Athens, 11527 Athens, Greece

<sup>2</sup> Biomedical Research Foundation, Academy of Athens, 11527 Athens, Greece

<sup>3</sup> Medical Physics Unit, 2nd Department of Radiology, Medical School, National and Kapodistrian University of Athens, Attikon University Hospital, 12462 Athens, Greece

<sup>4</sup> Section of Pharmaceutical Technology, Department of Pharmacy, School of Health Sciences, National and Kapodistrian University of Athens, 15771 Athens, Greece

<sup>5</sup> Laboratory of General Chemistry, School of Chemical Engineering, National Technical University of Athens, Zografou Campus, 15772 Athens, Greece

<sup>6</sup> School of Science and Technology, Hellenic Open University, 26335 Patra, Greece

\* Correspondence: nlagopati@med.uoa.gr; Tel.: +30-210-7462362

† These authors contributed equally to this work.

**Abstract:** Early-stage, precise disease diagnosis and treatment has been a crucial topic of scientific discussion since time immemorial. When these factors are combined with experience and scientific knowledge, they can benefit not only the patient, but also, by extension, the entire health system. The development of rapidly growing novel technologies allows for accurate diagnosis and treatment of disease. Nanomedicine can contribute to exhaled breath analysis (EBA) for disease diagnosis, providing nanomaterials and improving sensing performance and detection sensitivity. Through EBA, gas-based nano-sensors might be applied for the detection of various essential diseases, since some of their metabolic products are detectable and measurable in the exhaled breath. The design and development of innovative nanomaterial-based sensor devices for the detection of specific biomarkers in breath samples has emerged as a promising research field for the non-invasive accurate diagnosis of several diseases. EBA would be an inexpensive and widely available commercial tool that could also be used as a disease self-test kit. Thus, it could guide patients to the proper specialty, bypassing those expensive tests, resulting, hence, in earlier diagnosis, treatment, and thus a better quality of life. In this review, some of the most prevalent types of sensors used in breath-sample analysis are presented in parallel with the common diseases that might be diagnosed through EBA, highlighting the impact of incorporating new technological achievements in the clinical routine.

**Keywords:** breath analysis; disease diagnosis; nano-biosensors; sensors; volatile organic compounds; nanomaterials; cancer; diabetes; neurodegenerative diseases



**Citation:** Lagopati, N.; Valamvanos, T.-F.; Proutsou, V.; Karachalios, K.; Pippa, N.; Gatou, M.-A.; Vagena, I.-A.; Cela, S.; Pavlatou, E.A.; Gazouli, M.; et al. The Role of Nano-Sensors in Breath Analysis for Early and Non-Invasive Disease Diagnosis. *Chemosensors* **2023**, *11*, 317. <https://doi.org/10.3390/chemosensors11060317>

Academic Editor: Camelia Bala

Received: 12 April 2023

Revised: 17 May 2023

Accepted: 22 May 2023

Published: 24 May 2023



**Copyright:** © 2023 by the authors. Licensee MDPI, Basel, Switzerland. This article is an open access article distributed under the terms and conditions of the Creative Commons Attribution (CC BY) license (<https://creativecommons.org/licenses/by/4.0/>).

## 1. Introduction

Early, precise disease detection and design of the therapeutic scheme is a crucial topic with high scientific impact and has been over time. When these factors that are based on possibilities are considered by experienced scientists, the patients and the entire health system can benefit [1]. Due to the current rapid development of growing technologies, diagnosis and treatment might be easier. Owing to the growth of the population worldwide, the development of these fields has become even more important, and also leading to the creation of new areas, such as theranostics.

A great variety of sensor types have been developed over the years, having many biomedical applications. Various materials have been chosen to be used to modify the

sensors' properties, making them more effective. Accuracy, selectivity, sensitivity, and responsiveness are considered as parameters of paramount importance. In particular, functionality and performance are mainly related to the selected materials that might equip these sensors [2].

The accuracy of the diagnosis of multiple diseases currently requires a variety of clinical examinations, and of course expensive specialized equipment. In a primary care setting, when diseases are at their early stages and patients are asymptomatic or present non-specific symptoms, accurate diagnosis is not always possible given technical limitations [3]. Hence, the physician might, finally, approach the condition of the patient later than is optimal, which may eventually lead to the advanced-stage progression of the disease that makes a cure difficult. Therefore, many scientists focus their research on detecting diagnostic biomarkers and developing easy-to-use and portable devices that might provide a possible screening tool, and also a triaging system to risk stratify patients [4].

Taking into account the increased progress both in analytical techniques and nanotechnology, exhaled human breath analysis (EBA) has attracted great research and scientific interest, as it constitutes a non-invasive, real-time, and low-cost method for disease detection (e.g., for cancer, respiratory and kidney-related diseases, diabetes, and neurodegenerative diseases) and therapeutic and metabolic status monitoring [5]. This novel method is established primarily based on the analysis of the volatile organic compounds (VOCs) that are traced in the exhaled breath. This approach would potentially replace existing methods, such as blood test analysis, that are invasive and pain-inducing [6].

VOCs that are emitted through the exhaled breath are, actually, metabolites produced from different conditions and that are circulating through the vascular system. VOCs can be detected in the human breath via alveolar exchange [7]. Specifically, the process of breathing involves the transfer of the inhaled air to the lungs' alveoli, enabling the diffusion of the excreted (through metabolic procedures) products into the inhaled air [8,9]. The inhaled air, containing all of the discharged products, is then rejected as exhaled air. Thus, the exhaled air contains all of the crucial information regarding the endogenous metabolic processes taking place [8].

According to existing research, exhaled human breath primarily consists of nitrogen (~78%), oxygen (16%), hydrogen (5%), carbon dioxide (4–5%), inert gases (0.9%), and as water vapor [9]. Additionally, it contains inorganic VOCs, such as carbon monoxide (CO), nitric oxide (NO), nitrous oxide (N<sub>2</sub>O), ammonia (NH<sub>3</sub>), hydrogen sulfide (H<sub>2</sub>S), and organic VOCs, such as acetone (C<sub>3</sub>H<sub>6</sub>O), ethanol (C<sub>2</sub>H<sub>6</sub>O), ethane (C<sub>2</sub>H<sub>6</sub>), isoprene (C<sub>5</sub>H<sub>8</sub>), methane (CH<sub>4</sub>), pentane (C<sub>5</sub>H<sub>12</sub>), etc. [10].

Currently, more than 3000 VOCs have been listed as being detected in human exhaled breath, and are associated with disease-specific metabolic pathways. It is estimated that many of these VOCs contribute to pattern creation, aiding in the diagnostic process. It is worth mentioning that apart from the air that is exhaled, VOCs can also be detected in the urine, sputum, blood, and skin. However, among the aforementioned clinical samples, breath is easier to handle [11–13].

Moreover, the eminence of VOCs as biomarkers for various diseases is also affirmed by the fact that VOCs present noticeable and prompt variations during pathological conditions, modifying the typical biochemistry of the body through a separate or a combination of some of the following processes: oxidative stress, carbohydrate metabolism, liver enzymes, as well as lipid metabolism [14]. Some of the produced VOCs, appearing in normal, as well as abnormal cells, comprise mixtures of various compositions, while the rest of the VOCs are entirely derived from abnormal cells. Finally, each disease is characterized by a unique VOC pattern, thus facilitating diagnostic and therapeutic processes [7].

Sensors equipped with nanomaterials can be an effective tool in breath analysis for early, accurate and non-invasive disease diagnosis [15]. Due to the small dimensions of nanomaterials, their specific surface area (SSA) increases significantly, and thus even smaller amounts of molecules can become detectable [16]. Therefore, state-of-the-art nanosensors

for analyzing human breath have been developed by incorporating nanotechnology [17] (Figure 1).

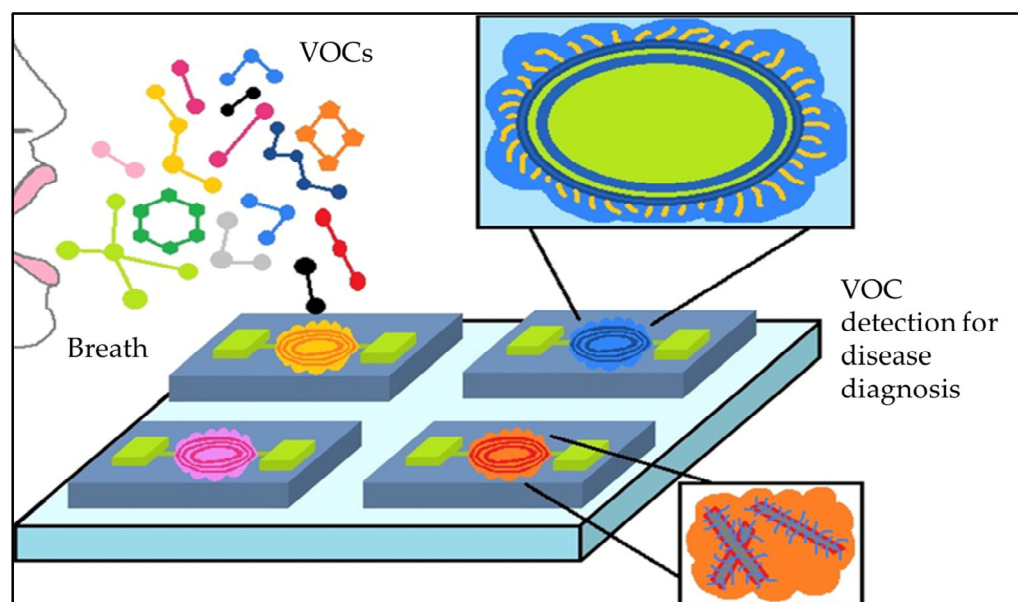


**Figure 1.** Representation of the process of breath analysis through nanosensors.

Despite the fact that the technology and the materials that are commonly used in sensor development have been continuously improved, there are still challenges that are essential to overcome [18–20], and thus prospects remain high. This comprehensive review systematically summarizes the recent developments in nanomaterials-based (NM-based) devices, as well as some of the most innovative nano-sensors that have been developed to detect various diseases. Furthermore, advanced technological and scientific challenges and future research endeavors have been discussed in depth in this research field, focusing on the importance of EBA becoming an integral part of every medical point of care and potentially a low-cost commercial tool that is widely available, can also be used as a disease self-test kit, highlighting the general impact of the incorporation of new technological achievements in the clinical routine.

## 2. Nanomaterials and Gas-Based Nanosensors

The utilization of innovative nanomaterial-based sensors for the accurate detection of biomarkers in breath samples has proven to be a promising research field for the non-invasive, precise and early diagnosis of several diseases. Therefore, nanomaterials can improve sensing performance and detection sensitivity in selective, cross-reactive applications [21].

Various types of nano-sensors have been developed, such as gas-based nanosensors, colorimetric nanosensors, electrochemical sensors, chemiresistors, piezoelectric sensors, and electronic noses, and have the potential to detect VOCs and can be used in breath analysis, demonstrating a relatively high sensing ability and responsiveness [22,23].

### 2.1. Surface Enhanced Raman Scattering

Surface Enhanced Raman Scattering (SERS) is an optical sensing method with various applications. Nanotechnology plays a crucial role, improving the essential parameters of this technique. SERS would be used as a gas analytical technique that is specialized to a single or a group of VOCs based on the Surface Plasmon Resonance (SPR) properties. The device is constructed with a porous material of which gas can pass through. The gases can be collected from different areas of the body, mainly through breathing [24]. In the study of Yang et al. a detecting platform was illustrated to gather SERS signals of gas-phase particles

by means of the improvement of a reasonable fluid that is dissolvable on the pinning-free substrate [25].

There are two major problems that have been reported with regard to all detection devices. The first is the difficulty in absorption on the surface of materials, and this is responsible for the low rates of detection due to the fact that gas molecules move with high velocities. Secondly, the Raman signals are undetectable in some gases due to their low concentration [26]. These problems can be overcome by modifying the morphology of the used nanomaterials or by combining nanoparticles of high affinity with the analyte molecules. This chemical modification may hopefully increase the retention time of the sample in the surface of the sensor and thus enhance the obtained Raman signals.

The detection of aldehydes is a characteristic example of lung cancer (LC) indicators. In particular, the development of cancer cells and their metabolism can lead to the production of a number of aldehydes that are exhaled and that are considered promising, especially in LC detection. Fuchs et al., after the measurement of aldehydes in the breath of cancer patients, healthy individuals, and smokers, indicated that certain aldehydes reflect angles of oxidative stress and tumor composition. As a result, certain aldehydes can be a biomarker for LC [27].

The difficulty of gases with regard to absorption on the surface of sensors, due to their relatively higher mobility, has already been mentioned. This problem can be easily solved when the commonly used gold nanoparticles (AuNPs) are coated with p-aminothiophenol, which is a Raman-active probe molecule that is selective to this substance (Figure 2) [24,28]. Moreover, in the study of Karakouz et al., the gas detecting capability of gold island based localized SPR (LSPR) transducers was investigated utilizing polymeric coatings as the dynamic interface. When gold island films are used for coatings of LSPR transducers, the final device appears vapor-dependent, and optical properties can be utilized for gas sensing [29]. Gas molecules are able to be entrapped on the cavities that are formed in proper nanomaterial morphologies, leading to the blockage of the gas flow (e.g., Ag-dendrimers detect aldehydes). When the analyte flows through the sensor, the strong interactions are continuously increasing on the remaining time of the gas [30]. These aggregates can cause electromagnetic enchantments and differentiate these molecules from the others of the sample, creating gaps in the spectrum.

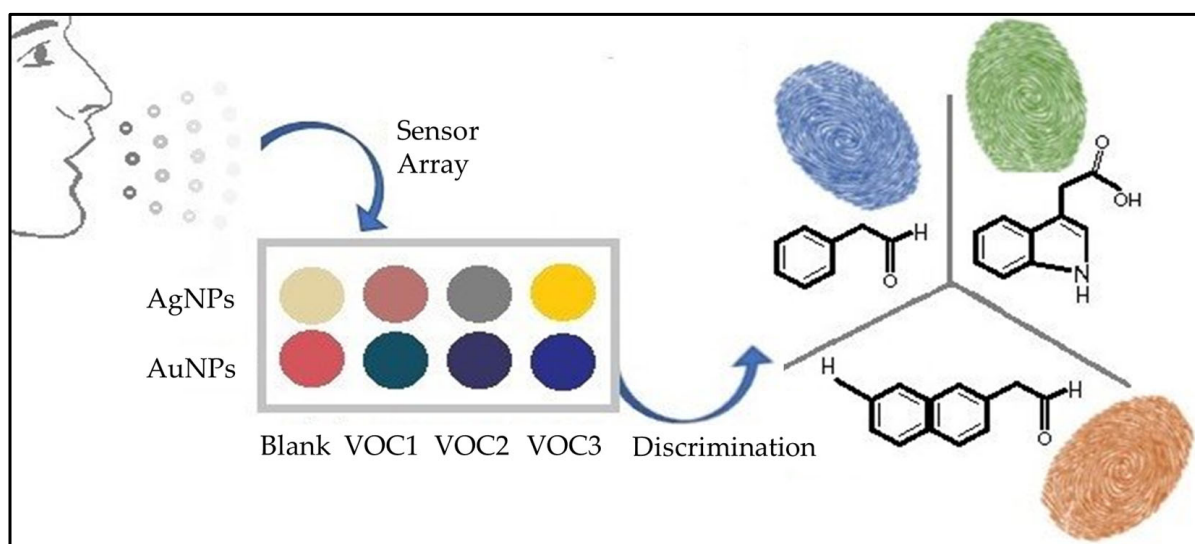


**Figure 2.** Aggregation of AuNPs modified with several substrates and the corresponding digital fingerprints.

## 2.2. Colorimetric Sensors

Colorimetric sensors are exploited in optical techniques, allowing cross-reactive detection, since they can identify multiple molecules simultaneously. The sensors of this type are

generally reliable and easy-to-use. For this reason, they can also be developed as wearable devices [31]. The fundamentals of these sensors are based on the optical changes that are observed in colorants. A great variety of dyes can be used for the determination of multiple compounds depending on their special affinity with the analyte.

AuNPs and Au nanorods (AuNRs) are considered to be ideal sensitive materials for building colorimetric sensors in biological system detection. Huo et al. used AuNRs-modified metalloporphyrins for the detection of VOCs that are considered as biomarkers of LC. They indicated that these nanomaterials enhanced their performance with regard to protecting the sensor device from degradation and improving their stability [32].

Colorimetric sensors can be developed with AuNPs. Thus, plasmon resonance wavelength alterations are measured and screened. Intermolecular forces are responsible for the effectiveness of the sensor. Hence, an efficient sensor is typically characterized by strong forces [31]. Colorimetric sensors can be structured with several materials that are able to be bound to the gas analytes. Some crucial factors such as humidity can affect the final outcome, since these interactions are, in general, weak. As a consequence, the main sensor characteristics such as responsiveness, sensitivity, and the limits of detection are weakened [33]. Therefore, it is clear that the stabilization of a sensor requires strong intermolecular forces. It is important to develop sensors using nanomaterials that form stronger bonds with the VOCs than Van der Waals bonds do. In particular, using chemically responsive dyes such as porphyrin to create colorimetric arrays can lead to the development of a precise application with a low limit of detection (LOD) (in scale of parts per billion) (ppb) [31] that can be applied to LC detection.

### 2.3. Electrochemical Sensors

Electrochemical sensors are a specific sensor type that is mainly specialized for the aldehydes, CO, and NO that exist in human breath. Actually, the electrochemical sensors consist of two electrodes and an electrolyte solution, thus creating a closed circuit. The concentration of VOCs that are measured is proportional to the productive current. Analytes create their own system: the electrochemical cell being based on their selective electrodes. Electrodes made of Au/Ag nanoparticle-coated multi-walled carbon nanotubes (MWCNTs) have the potential to be used in a system which is selective in terms of gas traces that are characteristic to stomach cancer [34]. Since this sensor type operates with a closed circuit, multiple cells can be connected in series, with each of them being selective for a specific compound. The main advantage of this sensor type is its ability to form complex structures, allowing the simultaneous analysis of several different VOCs and a powerful disease diagnosis [35].

Moreover, metal-organic frameworks (MOFs) nanoparticles have gained a significant amount of attention with regard to the advancement of commercial sensors. A study of Homayoonnia et al. showed that the use of  $[\text{Cu}_3(\text{TMA})_2(\text{H}_2\text{O})_3]_n$  in short (Cu-BTC) nanoparticles can create a sensor for VOCs detection. These NPs were examined as a dielectric layer of capacitive sensors for the location of different concentrations of acetone, methanol, ethanol, and isopropanol at the surrounding conditions. The outcome was the effective identification of these analytes with a high affectability at ppm concentration levels (among 250–1500 ppm). Diverse detecting behavior was observed towards methanol, isopropanol, ethanol, and acetone, showing that this sensor has great and sensible reaction times, great linearity, and a reversible reaction at different concentrations [36].

Generally, some parts of the devices and the analyzing gases form aggregations. This issue is associated with the sensor efficiency. Furthermore, among the measurements in a wide range of patients, a high fluctuation in the detected CO concentration has been reported, thus smoking has to be considered as a significant affecting factor [35]. In addition to the aforementioned issues, humidity is also a significant factor that should be taken into account. Specifically, when humidity is quite intense, it can affect the accuracy of the sample results [37]. Thus, sensors should be improved by utilizing inert materials,



particularly in those parts through which the gas moves in. Fortunately, humidity is a parameter that can be easily restricted by frequent calibration [37].

#### 2.4. Chemiresistors

Chemiresistors are another promising gas-based sensor type. Their simple design and the fact that they allow for easy and precise measurements are among their main characteristics. Generally, a semiconductor or metal sensing layer can connect the two sets of interdigitated electrodes. The sensor's resistance changes when exposed to gas, but the potential between the two electrodes still remains constant. The quantification of the analytes can be achieved through the calculation of the resistance/current change [38]. Various nanomaterial-based sensing films are used, such as nanotubes (NTs), graphene, carbon nanotubes (CNTs), nanowires (NWs), metal oxide semiconductors (MOS), metallic nanoparticles (MNPs), and hybrid nanomaterials for the detection of several diseases. Two main categories are considered: MOS-based and carbon-based chemiresistors (Figure 3).

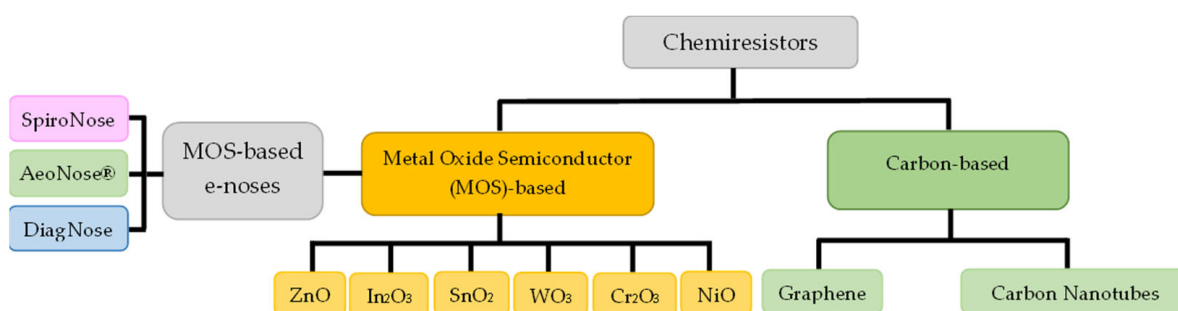


**Figure 3.** The main categories of chemiresistors and the three common MOS-based e-noses for LC and the detection of other diseases.

##### 2.4.1. MOS-Based Chemiresistors

Owing to their low-cost and simple manufacture, portability, and high sensitivity to gases [39], among those gas sensing materials, MOS (e.g.,  $\text{In}_2\text{O}_3$ ,  $\text{ZnO}$ ,  $\text{SnO}_2$ ) and particularly transition MOS (e.g.,  $\text{Cr}_2\text{O}_3$ ,  $\text{WO}_3$ ,  $\text{NiO}$ ) are considered as ideal options for resistive gas sensors. MOS chemiresistors can detect oxidizing/reducing gases [31]. The high-temperature operation that is incompatible with wearable sensing technology in parallel with the lack of selectivity towards gases are considered to be the main drawbacks of these sensors. The development of MOS nanostructures or other sensitive materials could improve the selectivity of the MOS-based sensors. For instance, the combination of  $\text{In}_2\text{O}_3$  with  $\text{NiO-In}_2\text{O}_3$  gas sensors have an excellent response time [40]. Two-dimensional materials such as graphene can be combined with metal oxide producing gas-sensitive reactions at room temperature (RT) [39].

##### 2.4.2. Carbon-Based Chemiresistors

Carbon-based nanomaterials (e.g., graphene, carbon nanotubes (CNTs)) have been studied for the development of gas-sensor-wearables [41,42], due to their physicochemical properties, RT-sensing ability, and also their compatibility with other nanomaterials for enhanced performance [41,42]. In particular, graphene and its derivatives, such as graphene oxide have been found to be great at detecting execution and are promising gas-sensitive materials. This is due to their amazing particular surface region ( $2620 \text{ m}^2/\text{g}$ ), great thermal resistance (oxidation resistance  $650^\circ\text{C}$ ), and high carrier portability ( $2 \times 10^5 \text{ cm}^2/\text{Vos}$ ). Numerous oxygen-containing bunches on the surface of graphene and its subsidiaries give them a crucial gas adsorbing ability through the polar effect. When adsorbing gas, the ventured distinction is in resistance. Graphene can alter its electronic scattering and cause a resistivity contrast caused by distinguished gasses. An electron acceptor such as nitrogen

dioxide, water, etc. and an electron benefactor such as ethanol or ammonia will appear with diverse responsiveness characteristics [37].

Single-walled carbon nanotubes (SWCNTs)-based sensors have demonstrated a better response compared to MWCNTs [42]. CNT sensing can be derived through the adsorption of gas molecules onto the CNT surface, through van der Waals attraction, leading to significant alterations in electrical conductivity [43]. The reduced chemical selectivity is among the major limitations that is met in the applications of CNTs-based sensors [14]. The selectivity and sensitivity can be improved when chemical modification of CNTs using MNPs, polymers and metal oxides is conducted [38]. SWCNTs that are coated with Au NPs which can enhance the sensitivity [44].

### 2.5. Piezoelectric Sensors

Voltage is created when mechanical stress is applied on to the surface of the sensitive layer of piezoelectric materials [45]. Quartz crystal microbalance (QCM) is a representative category of this sensor type.

#### Quartz Crystal Microbalance Sensors

QCM-balance is a commonly used piezoelectric sensor that is used for gas detection [42]. The absorption of targets on the surface of the crystal, upon sensor exposure to a breath sample, can cause significant changes in mass and resonant frequency [46]. Various sensing materials such as MOS, metalloporphyrins, polymers, and nanomaterials can functionalize the quartz crystal resonator [47,48]. Creating coatings on these sensors by using chemical layers that are sensitive to acetone, such as ZnO, WO<sub>3</sub>, SnO<sub>2</sub>, and In<sub>2</sub>O<sub>3</sub>, can enhance their sensitivity [42]. If rhodium is added to the hollow WO<sub>3</sub> spheres, it can improve the selectivity for acetone, decreasing the impact of humidity [49]. The ability of a QCM sensor to monitor the target analytes in real time [42], in addition to its high sensitivity and low power operation [48], are among those characteristics that make them very useful.

Ahmed et al., in 2019, developed a sensor device with polymer-coated piezoelectric micro-cantilevers for the determination of VOCs. They portrayed a sensor gadget with a cluster of eight polymer-coated piezoelectric micro-cantilevers and an electronic thunderous recurrence readout, outlined for the investigation of VOCs. Three of these polymers were capable of distinguishing between VOCs [50]. Although this study showed that a low-cost micro-cantilever sensor is able to identify VOCs, extra experimental efforts need to be undertaken in order to overcome the limitations, such as the lack of selectivity. In future studies, Ahmed et al. propose an improved gas conveyance setup where VOCs are tested in water, since the breath is humid, with regard to the analysis of VOCs, in order to monitor the impact of stickiness on VOC separation. By using synthetic air rather than N<sub>2</sub> CO<sub>2</sub> can break up the humidity [50].

### 2.6. Electronic Noses

When it is unclear as to what kind of VOCs are present, or when there is a wide range of existing compounds, is better to try a semi-selective sensing approach by using an e-nose system. Electronic noses (e-noses) have been developed allowing for the accurate measurement of VOCs by combining diverse materials with several non-selective gas sensors in a single array, and thus exploiting pattern-recognition algorithms [46]. These technologies are based on different fundamentals and use different sensing materials and array composition [51]. The e-nose sensor can mimic the human nose, identifying gases based on their chemical composition [46]. To improve performance, different functionalizations should be used [52].

An e-nose system can typically employ a sensor array to detect various gases, but the traditional MOS sensors used in these arrays consume high amounts of power and are not flexible in adjusting their sensitivity and selectivity. QCM sensors, on the other hand, offer advantages such as low power consumption, real-time detection, and the easy modification of their sensing surfaces to tune their sensitivity and selectivity. QCM sensors can be coated

with different materials, both inorganic and organic, but polymers are particularly popular due to their versatility in adjusting their chemical and physical properties [53]. In addition, research has shown that the integration of electrospun nanofibers as active materials in QCM-based gas sensors is effective [54].

Piezoelectric and chemiresistive sensors are typically used in cross-reactive devices and sensor arrays. Several nanomaterials such as graphene, CNTs, MNPs, MOS, metal monolayer-capped nanoparticles (MCNPs), as well as polymers have been used as components of e-noses. If these nanomaterials are modified or combined with others, this leads to the development of hybrid materials, broadening the range of their applications [46], improving their cross-selectivity and sensitivity [48], and allowing for accurate pattern detection. The size of the nanomaterials makes them well-suited for medical breath testing, as they closely match the dimensions of typical breath VOCs [55]. By combining nanobased sensors with artificial neural network analysis, enhanced diagnosis accuracy can be achieved [56].

MOS-based chemiresistors (e-noses) possess high accuracy and specificity in the detection of LC and other diseases, at RT [48]. The main types of e-noses are the SpiroNose [57], aeoNose [58], and DiagNose [59], and are presented in Figure 3. Furthermore, chemiresistor-based MCNPs are considered as very promising for the detection of VOCs. Pt or Au MCNP deposition using the layer-by-layer technique can reduce the humidity effect [60]. Due to their ability to function at RT, in addition to their excellent sensitivity and selectivity, polymers are employed in commercially available e-noses [47]. E-noses that were constructed using eight QCM coated with metalloporphyrins succeeded in effectively identifying 94% of LC cases [47].

### 2.7. Surface Modification of Sensors

Different nanomaterials with unique sensing properties, such as MOS, CNTs, graphene-based materials, and polymers, are used as sensing materials. For example, MOS sensors loaded with catalysts have been utilized for detecting diabetes. Additionally, metal ion composites with metal MOS-based sensors have shown the ability to selectively detect VOCs associated with lung cancer. A gold nanoparticle-based sensor array can also be considered as a technique for detecting cancer VOCs from the breath. This category of nanomaterials can be customized with different materials to detect specific gases with high accuracy [61].

Monolayer-capped gold nanoparticle (monolayer-capped GNP) sensors are a cost-effective solution with several advantages, including the extremely precise detection of VOCs (as low as sub-ppb), a broad detection range, compatibility with normal room conditions, and resistance to background molecules such as humidity. These benefits stem from the ability to tailor the physical-chemical properties of the monolayer-capped GNPs to meet specific sensing requirements. By adjusting the organic ligand or the shape of the GNPs, and incorporating advanced software algorithms, many confounding factors (such as gender, age, ethnicity, and smoking habits) have been effectively eliminated [62].

The modification of CNT sensors results in enhanced performance. By adding different materials, such as conductive polymers or metal nanoparticles, sensors become more sensitive and selective than regular CNT sensors. Functionalized CNTs are a great option for creating compact gas sensors and arrays with a high sensing capability [63].

Organic functionalization is a useful method for detecting different types of VOCs by providing unique adsorption sites [55].

## 3. Nanosensors for Disease Diagnosis through Exhaled Breath Monitoring

### 3.1. Diabetes and Diagnosis Using Nanosensors

Diabetes constitutes a group of severe, chronic metabolic disorders, related to increased blood glucose levels, leading to enhanced rates of premature morbidity. Despite the fact that quality of life is increasing, diabetes has not yet shown a downward trend. On the contrary, it continuously burdens health systems worldwide [64]. Diabetes is often diagnosed



when irreparable organ damage has already occurred due to prolonged hyperglycemia. Thus, diabetes comprises one of the highest public health challenges worldwide [64], along with cancer and chronic respiratory and cardiovascular diseases, leading to approximately five million deaths annually in developed countries, mainly from cardiovascular disease (50%) and kidney failure (10–20%). Diabetes is also responsible for blindness, lower limb amputations, and severe complications of viral infections, such as COVID-19 [65]. Its main types are: (a) insulin dependent or juvenile diabetes (T1DM—Type 1 Diabetes Mellitus); (b) non-insulin dependent (T2DM—Type 2 Diabetes Mellitus); and (c) gestational diabetes [66]. Additionally, more infrequent types are also detected as a result of other causes, also including diseases of the exocrine pancreas, a genetic defect of  $\beta$ -cell function or insulin action, endocrinopathies, and drug or chemical-induced diabetes [67].

T1DM is caused by the inferior production of insulin in the pancreas due to autoimmune  $\beta$ -cell destruction [65]. It accounts for about 10% of the diabetes diagnosed types [68]. Predominant factors causing its emergence include the environment (including viruses, bacteria and pollutants), nutrition, and genetic factors [65]. At an advanced stage of T1DM, patients exhibit severe insulinopenia as insulin production almost ceases, and this causes hyperglycemia [66]. Exogenous insulin therapy is thus necessary in order to maintain a basic level of insulin, prevent complications due to disease, and maintain life [66]. In the case of T2DM, the cause lies in peripheral insulin resistance, corresponding to inadequacies in the cellular response to insulin [66]. T2DM is the predominant type, accounting for almost 80–85% of total diabetes cases [69]. The increased frequency of T2DM is primarily due to a sedentary lifestyle, obesity, and a genetic predisposition [70], while it is also related to hypertension and dyslipidaemia [65]. In order to accomplish good metabolic control and delay T2DM, a combination of lifestyle alterations, such as dietary intake and exercise, and finally pharmacological (injectable and/or oral drugs) treatment, is necessary for improving not only insulin production but also its function [71,72]. As for the third type of diabetes, it is defined as any level of glucose intolerance, starting in or being initially detected during pregnancy [66]. It is usually diagnosed in the second or third trimester of a pregnancy due to high blood glucose levels [73] in cases where pancreatic function in women is not sufficient to monitor the diabetogenic environment during pregnancy [74].

Diagnosis constitutes the initial critical part of diabetes control and handling. So far, a diabetes diagnosis is conducted through conventional methods, such as the analysis of fasting plasma glucose (FPG) levels, or the oral glucose tolerance test (OGTT), as well as hemoglobin A1c (HbA1c) levels [75,76]. Nevertheless, these methods are found to be painful by the majority of patients because of the injection during the blood withdrawal. Next to the fact that these methods are uncomfortable and lead to patients' therapy neglect, periodic measurements may not detect large variations in the glucose level happening between points of measurement. Furthermore, the measured value presents alterations owing to various factors, including the time of testing age and the extant physiological condition. These methods are also not appropriate for the continuous monitoring of diabetic patients due to the exhausting process, long time to diagnosis, increased amount of venous blood withdrawal, as well as whole blood processing [77]. Most importantly, potentially harmful diabetes symptoms, such as hyperglycemia, are clinically noticed after disease progression, thus prohibiting early interference. It is important to find cheaper, quicker, and more widely available diagnostic tools in order to avoid the severity of these complications.

In order to confront, as well as overcome, the aforementioned complications, different types of nanotechnologies, based on exhaled breath analysis and various biomarkers, have been developed recently for the enabling of the earlier and non-invasive detection of diabetes. The specific biomarkers traced in the exhaled breath are used to indicate a variety of diseases [78].

Acetone comprises the most commonly accepted diabetes biomarker that is found in the breath and that is not importantly affected by the mouth flora [79]. Acetone was initially delineated as a diabetes' breath biomarker by Petters in 1857 [6]. Figure 4 summarizes the historic order of the measure of acetone.

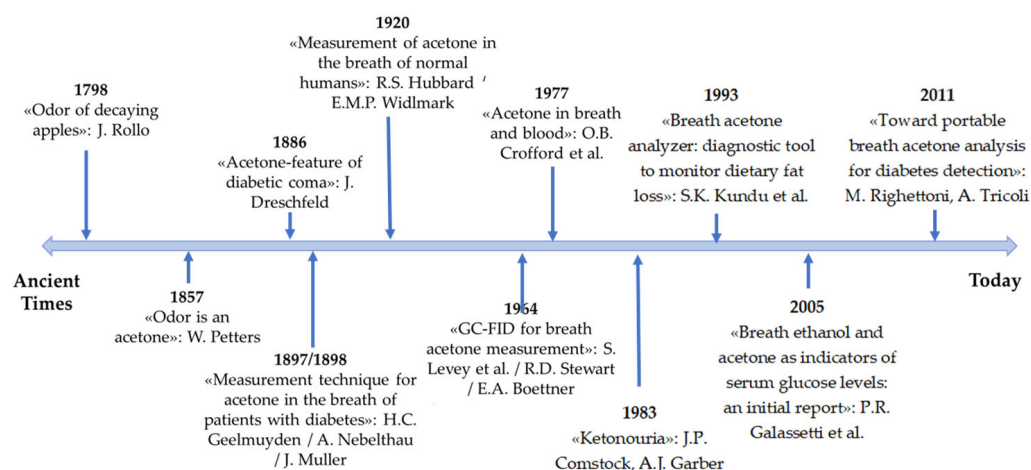


**Figure 4.** Acetone measurement through the years (Based on [78]).

Glucose constitutes the primal energy source in the human body, and is absorbed into the cells with the assistance of insulin. In the case of T1DM and T2DM, the human body does not possess the ability to produce energy from glucose; in contrast, energy production is accomplished through the body's fat decomposition [80]. Ketogenesis constitutes one of these pathways, as well as the source of all ketone bodies, including acetone, in the human body. The acetone concentration in the breath becomes enhanced as the severity of diabetes escalates. Patients with diabetes also tend to present enhanced aldehyde levels in both blood and breath samples [81]. Moreover, diabetes may develop due to metabolic as well as genetic disorders during the synthesis and metabolism of aldehydes, such as methylglyoxal, glyoxal, semialdehydes, formaldehyde, etc. [82]. According to other studies, exhaled isoprene, isopropanol, pentanal, carbon monoxide, methyl nitrate, and dimethyl sulfide levels were found to be increased in T1DM patients [83], while T2DM patients were found to have elevated levels of ethylene, carbon monoxide, isopropanol, ammonia, toluene, 2,6,8-trimethyldecane, 2,3,4-trimethylhexane, and tridecane in exhaled breath samples [84].

#### Nanotechnology and Nanobiosensors for Diabetes Diagnosis

Nanotechnology has opened up new frontiers and perspectives for the development of unique, innovative sensors for the exhaled breath analysis for the detection of diabetes. Metal-based nanosensors (MOXs) have been thoroughly studied, detecting VOCs, and especially acetone, through EBA, due to several advantages, such as their compact size, facile production, low cost, as well as simple measurement using electronics [78].

SnO<sub>2</sub> has gained the greatest and most extensive attention among all MOXs, owing to its enhanced sensitivity, selectivity, and stability, as well as its rapid response and recovery times. SnO<sub>2</sub> constitutes an n-type semiconductor characterized by a decreasing resistance under the influence of a reducing gas. It is worth mentioning that the relatively increased optimum temperatures comprise one of the principal limitations of SnO<sub>2</sub>-based sensor devices for biomedical applications [78]. As a result, in order for the limitations to be vanquished, several dopants, such as Pt [85], Au [86], Pd [87], CNTs [88], and graphene oxide (GO) are often added to SnO<sub>2</sub>. Several studies focused on the development of SnO<sub>2</sub>-based sensors, and some of the most representative ones are summarized in Table 1.

**Table 1.** SnO<sub>2</sub>-based sensors and their performance in acetone selection for diabetes diagnosis.

Material Used for the Development of SnO <sub>2</sub> -Based Sensors	Results	Ref
Ca <sup>2+</sup> / Au co-doped SnO <sub>2</sub> nanofibers	Enhanced sensing performance against acetone at 180 °C	[86]
Thick film sensors consisting of Pd loaded Sn-doped SnO <sub>2</sub>	Increased response equal to 81% towards 25 ppm acetone concentration at 200 °C. Fast response/recovery	[87]
MWCNTs/SnO <sub>2</sub> nanocomposites	Excellent selectivity, stability, and reproducibility Significantly enhanced response towards acetone (0.5–5 ppm)	[88]
SnO <sub>2</sub> nanofibers/rGO nanosheets	High sensitivity towards acetone Limit of detection: 100 ppb acetone at 350 °C	[89]
Flower-like pristine SnO <sub>2</sub> and NiO/SnO <sub>2</sub> hierarchical nanostructures	Very good acetone sensing performance at 300 °C Temperature-dependent dual selectivity for detecting both formaldehyde (110 °C) and acetone (250 °C).	[90]
Pd-Au bimetallic nanoparticles decorated SnO <sub>2</sub> nanosheets	Increased response, recovery time, and great selectivity under their optimum operating temperature. The ability to detect ultra-low concentrations of acetone in high RH (relative humidity) environments (94%).	[91]

Zinc oxide (ZnO) constitutes one of the most promising MOXs used for applications related to gas sensing. ZnO has been widely utilized since the 1960s, and for this reason the gas sensing mechanism is well established. Nevertheless, novel types of zinc oxide doped and/or decorated nanostructures have been increasingly studied for acetone detection at extremely low concentrations [92]. Table 2 presents a representative study focusing on ZnO sensors and their properties against acetone detection for diabetes diagnosis.

**Table 2.** ZnO-based sensors and their performance in diabetes diagnosis.

Material Used for the Development of ZnO-Based Sensors	Results	Ref
Novel hierarchical ZnO nanoparticles	Increased gas sensing performance, sensitivity, and response towards acetone	[93]
Au-modified flower-like hierarchical ZnO nanostructures	Significantly increased response to acetone in comparison to bare nano-ZnO or non-modified flower-like hierarchical ZnO nanostructures. Limit of detection: 0.5 ppb Successful acetone detection at 310 °C.	[94]
ZnO-CuO hybrid composites	Improved response, good resolution under low concentrations. Limit of detection: 100 ppb	[95]
ZnO thin-films	High response and selectivity towards acetone. Limit of detection: 2 ppm at room temperature. High-performance sensing materials towards acetone.	[96]
novel double-shelled ZnO hollow microspheres	Increased sensitivity, response/recovery time, stability, and selectivity towards acetone. Limit of detection: 0.5 ppm	[97]
Pt decorated Al-doped ZnO nanoparticles	Superior sensing performance under exposure to 10 ppm acetone (450 °C).	[98]
Al, Cu and Co doped ZnO nanoparticles	Al-doped ZnO nanoparticles presented the most increased response during the exposure to acetone (1 ppm at 500 °C). Limit of detection: 0.01 ppm at 90% humidity.	[99]

Tungsten oxide ( $\text{WO}_3$ ) is considered as a typical n-type material for gas-sensing that has also attracted considerable attention for the possible detection of various gases, acetone being among them. The  $\text{WO}_3$ -based acetone sensors  $\text{WO}_3\text{-Cr}_2\text{O}_3$ ,  $\text{Si:WO}_3$  are suitable for acetone detection, since they rapidly respond to short breath pulses [100]. Some characteristic studies that are devoted to the investigation of  $\text{WO}_3$ -based acetone sensors are presented in Table 3.

**Table 3.**  $\text{WO}_3$ -based sensors and their properties in diabetes diagnosis through EBA.

Material Used for the Development of $\text{WO}_3$ -Based Sensors	Results	Ref
C-doped $\text{WO}_3$ poly-crystalline sensor	Enhanced response, rapid recovery at an acetone concentration range 0.2–5 ppm at 300 °C. Adequate long-term stability. Capability of discerning healthy persons (<0.9 ppm) and diabetic patients (>1.8 ppm), at 95% relative humidity.	[101]
Gd-doped $\text{WO}_3$ /RGO nanostructures	Enhanced response (54) towards 50 ppm acetone at 350 °C.	[102]
monoclinic $\text{WO}_3$	Limit of detection: 7.5 ppb	[103]
PtCu/ $\text{WO}_3\cdot\text{H}_2\text{O}$ hollow spheres	Enhanced sensitivity, efficient selectivity rapid response/recovery speeds, ultra-low detection limit (0.01 ppm), and good stability.	[104]
3D inverse opal (3DIO) $\text{WO}_3$ /Au	Increased response and selectivity towards acetone. Limit of detection: 100 ppb.	[105]
PdO/ $\text{WO}_3$ core-shell	Enhanced response (equal to 40) towards 50 ppm acetone.	[106]
$\text{Sb}_2\text{O}_3$ / $\text{WO}_3$ yolk-shell	High sensitivity, increased selectivity towards acetone, stability up to 2 months. Enhanced response (equal to 50) towards 100 ppm acetone.	[107]
Nb-doped ferroelectric $\epsilon\text{-WO}_3$ spheres	Enhanced acetone's surface reaction due to ferroelectricity. Rapid response time.	[108]
2D $\text{WO}_3$ nanosheets	Ultra-low limit of detection: 8.9 ppb Increased response (14.7–50 ppm of acetone) Extremely low limit of detection (ppb level). Adequate selectivity towards other VOCs Rapid response/recovery rates (6/9 s to 0.17 ppm of acetone)	[109]
Pd/ $\text{WO}_3$ nanostructures	Good repeatability (100 cycles) Long-term stability (14 days) Low-cost, reliability, repeatability. Remarkable acetone response at 20–1000 ppm, at room temperature.	[110]
Pt-decorated $\text{NiWO}_4$ / $\text{WO}_3$ nanotubes	Enhanced selectivity, good stability. Supreme response at 375 °C towards acetone sensing.	[111]
Ru-Pd/ $\text{WO}_3$	Excellent stability and selectivity Selectivity, increased stability, rapid response/recovery times. Ultra-high sensitivity (~99.80%) at 10 ppm acetone.	[112]

Table 3. Cont.

Material Used for the Development of WO <sub>3</sub> -Based Sensors	Results	Ref
Fe-doped reduced graphene oxide (rGO) decorated WO <sub>3</sub>	Excellent selectivity, adequate reproducibility and stability. Limit of detection: 1 ppm	[113]
Various morphologies of WO <sub>3</sub> (spheres, nanorods, flowers and sea urchins)	The sea urchin morphology was the best choice. Supreme stability and sensitivity. Selective and rapid response to acetone concentrations 2–5000 ppm at 200 °C.	[114]
0.5% PtO-WO <sub>3</sub> nanofibers	Excellent sensing performance at 260 °C. Acceptable stability and selectivity towards the acetone biomarker.	[115]

Graphene comprises a two-dimensional carbon nanomaterial characterized by an increased aspect ratio and a specific surface area, as well as supreme electronic properties that have garnered significant attention since its discovery. Both graphene and its derivatives, such as graphene oxide (GO) and reduced graphene oxide (rGO), have demonstrated an adequate sensing performance towards acetone gas. Some representative studies are presented in Table 4.

Table 4. Graphene-based sensors and their performance in diabetes diagnosis.

Material Used for the Development of Graphene-Based Sensors	Results	Ref
rGO-Se nanocomposite	Advanced response towards 100 ppm of acetone at 135 °C. Fast response/recovery times and good reproducibility.	[116]
ternary FeCo <sub>2</sub> O <sub>4</sub> /graphene hybrid nanocomposite	Increased sensitivity towards acetone gas.	[117]
reduced graphene oxide (rGO) and rGO-rosebengal (RB) composites	rGO-RB composite indicated the most enhanced response. (1.6% to 3.2% for 1000 and 2000 ppm of acetone, respectively) at room temperature	[118]
decorated graphene with Ag <sub>2</sub> S nanoparticles	Sufficiently enhanced response.	[119]
Ag nanoparticles modified Fe <sub>3</sub> O <sub>4</sub> /rGO composites	Selectivity and sensitivity towards acetone.	[120]
AuNPs decorated vertical graphene nanosheet composites	Excellent selectivity to acetone. Acetone detection at 140 ppm at room temperature. Rapid response time (300 s). Adequate recovery time (152 s).	[121]

Indium oxide (In<sub>2</sub>O<sub>3</sub>) is broadly used in microelectronics, including gas sensors. However, the sensing performance of these gas sensors relies on their fabrication approach, which ascertains the phase composition, the atomic structure's formation, as well as indium's electronic states within the sensor material. The main results obtained from studies focusing on In<sub>2</sub>O<sub>3</sub>-based sensors are presented in Table 5.



**Table 5.** In<sub>2</sub>O<sub>3</sub>-based sensors and their potential in diabetes diagnosis.

Material Used for the Development of In <sub>2</sub> O <sub>3</sub> -Based Sensors	Results	Ref
Fe <sub>2</sub> O <sub>3</sub> -functionalized In <sub>2</sub> O <sub>3</sub> nanowires	Responses ranging from 298 to 960% to acetone concentrations 10–500 ppm at 200 °C.	[122]
sub-spherical Pt-In <sub>2</sub> O <sub>3</sub> nanoparticles	Exceptionally low detection limit (10 ppb)	[123]
SnO <sub>2</sub> /Au-doped In <sub>2</sub> O <sub>3</sub> core-shell nanofibers	High response (at 300 °C) Rapid response and acceptable selectivity towards acetone gas. Ideal operating at 300 °C,	[124]
α-Fe <sub>2</sub> O <sub>3</sub> -In <sub>2</sub> O <sub>3</sub> heterostructure nanocomposites	Enhanced response (37) at acetone concentration 20 ppm compared to bare material (about seven times greater).	[125]
Pd sensitized mesoporous In <sub>2</sub> O <sub>3</sub> nanocomposites (1.0, 1.5 and 2.0 mol% Pd-loading amount)	Noticeable sensitivity, selectivity, MS, and response for acetone gas (50 ppm) of the 1.5 mol% Pd-loaded In <sub>2</sub> O <sub>3</sub> .	[126]
1D porous Pt-doped In <sub>2</sub> O <sub>3</sub> nanofiber structures	Increased sensing response towards acetone Limit of detection: 10 ppb at 180 °C. Fast response/recovery time.	[127]
In <sub>2</sub> O <sub>3</sub> /MWCNT	Enhanced selectivity towards acetone. Adequate reversibility and time stability (50 days). Increased sensing performance.	[128]
In <sub>2</sub> O <sub>3</sub> nanowires	Limit of detection: 10 ppm at 300 °C. Increased response (37.9) at 100 ppm of acetone at 200 °C.	[129]
In <sub>2</sub> O <sub>3</sub> /ZrO <sub>2</sub> composite	Fast response/recovery time. Good response for 100 ppm of acetone.	[130]
a flower-like WO <sub>3</sub> -In <sub>2</sub> O <sub>3</sub> hollow heterostructure	Concise response time (1 s) at 260 °C. Advanced sensing performance towards acetone.	[131]

Except for the vastly utilized MOXs, various other materials have been examined and/or used as sensing materials towards acetone gas. In 2021, Das et al. [132], developed a highly sensitive and stable cobalt chromite (CoCr<sub>2</sub>O<sub>4</sub>) thick film designed to serve as a trace acetone sensor, characterized by rapid response/recovery times and therefore to be used as a diabetes detector used for exhaled human breath. Jiang et al. [133] reported the fabrication of a stabilized zirconia (YSZ)-based acetone sensor combined with a Cd<sub>2</sub>SnO<sub>4</sub> sensing electrode in order to be tested for its potential to act as a pre-diagnostic tool for diabetes. The as-synthesized sensor could successfully detect acetone in very low concentrations (0.05–200 ppm) at 600 °C, while it was characterized by exceptional repeatability, selectivity, and stability, making it a reliable candidate for real-life applications. In 2022, Verna et al. [134], synthesized a perovskite BaSnO<sub>3</sub>-based acetone sensor for detecting very low acetone concentration in human breath through a sol–gel method. The sensor indicated the most increased sensing response for 50 ppm of acetone at 80 °C, and also demonstrated an exceptional linearity between blood glucose levels and the response. Parmar et al. (2022) [135], used a polymer-modified sensor array, consisting of three sensors, in order to detect acetone concentrations ranging from 5 to 400 ppm. Moreover, data derived from the acetone sensor combined with individuals' breath samples were exploited in order to distinguish individuals with no diabetes history, diabetic patients, and high metabolic rate individuals (e.g., people with more than average physical activity). The team emphasized that the as-developed sensor array, in addition to the use of a neural network, would be able to detect diabetes cases at an accuracy greater than 90%. Lastly, Zhang et al. [136], examined a SmFeO<sub>3</sub>-based sensor, developed via a sol–gel approach, to be utilized as a detector of acetone gas in exhaled human breath. The sensor indicated excellent responses towards acetone within the concentration range 0.1–1 ppm, while its selectivity and relative humidity adaptability was exceptional.

### 3.2. Nanobiosensors for Cancer Diagnosis

#### 3.2.1. Diagnosis of Lung Cancer

Lung cancer (LC) is among the most common cancers that is responsible for millions of deaths worldwide. It is a type of cancer whereby, due to its symptoms (or the general absence of them) diagnosis occurs at later stages, with treatment being a challenge. As a result, a fast and accurate diagnostic method is required. The common diagnostic tools include a chest X-ray, low dose computed tomography (CT), analysis through sputum cytology, bronchoscopy, and other biopsies of nodules or on a suspicious mass of the tissue [137]. However, apart from their paramount importance, some drawbacks of these techniques make them challenging for systematic use. Furthermore, specialized personnel are required to perform them. In addition, some biosignatures associated with tissue functions are detected in parallel with the aforementioned methods to ensure the diagnostic result (protein markers VEGF, CD59, etc.), genetic markers (RASSF1A, K-ras mutant, p53 mutant, etc.) [138], but occasional unreliable results contribute to difficulties in LC diagnosis. Thus, alternative diagnostic methods are highly suggested, and EBA is a very promising choice. Among the main advantages of EBA for LC diagnosis are the following: (a) the simplicity of the breath specimen; (b) the specimen collection process; (c) the low-cost production; (d) the portability of the EBA sensors; and (e) the fact that it is a noninvasive method.

VOCs exhaled from patients suffering from different types of cancer disease are often similar. Fortunately, in some cases, specific gases are detected, allowing for the diagnosis of each cancer type. In particular, specialized metabolic processes which appeared in LC cases released unique products that might be considered as strong indicators for accurate LC diagnosis [139]. Among the metabolic products, the volatile compounds or the molecules that are insoluble to blood can escape through breathing and can be exploited as biomarkers [139]. Aldehydes, aromatic derivatives, hydrocarbons, and alcohols are the most common compounds in LC cases. In particular, aldehydes arising from the metabolic process of their corresponding alcohols are supported from ADH and ALDH enzymes and are considered as markers of carcinogenesis. Hexanal and acetaldehyde are associated with oxidative stress and DNA damage, respectively. Benzene, toluene, and 2,5-dimethylfuran are related to smoking, and are found as the components of tobacco in LC patients. The significant fluctuation in alcohol concentrations is observed in LC cases. Lung cancer cells typically produce 2-ethyl-1-hexanol [140]. Some of the most characteristic markers of LC are presented in Table 6.

**Table 6.** Volatile Compounds in LC.

VOC	Production Mechanism	Ref
Saturated Hydrocarbon (aldehyde, ethane, pentane, etc.)	Lipid peroxidation of lipids of the cellular membrane, due to oxidative stress	[141]
Oxygen-containing (acetone, etc.)	Lipolysis or lipid peroxidation	[141]
Unsaturated hydrocarbon (isoprene, etc.)	Cholesterol synthesis pathways	[142]
Nitrogen-containing (ammonia, etc.)	Liver impairment and Uremia	[143]
Sulfur-containing (dimethylsulfide, etc.)	Incomplete methionine metabolism	[144]

#### 3.2.2. Nanobiosensors for Lung Cancer Diagnosis

There are plenty of sensors for LC detection. The sensors that show higher accuracy and sensitivity are mentioned below [45]. To begin with, sensors should be multifunctional, consisting of separate arrays. Each of them should be designed in order to be selective with a specific group of exhaled compounds. The identification of biosignatures or patterns requires the simultaneous detection of various VOCs. Thus, their structure is quite complex given the necessary calculation of different vectors combining the arrays leading to the final result, but their impact is significant [145].

Nanomaterials play an important role in these types of sensors as their use in the development of nanosensors can further improve the diagnostic field of EBA [138]. In

particular, due to the unique properties of nanoparticles, they can improve the sensing performance in terms of the accuracy, sensitivity, limit of detection, and selectivity. Several studies that applied combinations of arrays and analytes indicated very promising results with regard to their reliability. The study of Binson et al. was characteristic. They used a detection device consisting of five sensors (TGS 822, TGS 826, TGS 2600, TGS 2610, and TGS 2620) [146]. Specifically, TGS 2600 could detect ethanol, methane, isobutane, and CO (1–100 ppm), while TGS 2610 was able to detect ethanol, propane, methane, and isobutane (300–10,000 ppm). TGS 2620 targeted CO, ethanol, isobutane, and methane (50–5000 ppm), while TGS 822 could detect acetone, benzene, ethanol, and methane (50–5000 ppm), and TGS 826 detected ethanol, ammonia, isobutane, and hydrogen (30–300 ppm) [146]. This e-nose system provided a sampling frequency of 8 Hz, a sampling time of 120 s, a sample injection flow rate of 60 mL/s, a sensor array chamber capacity of 80 mL, and is presented in Figure 5. Among 32 LC patients, 38 of them suffering from chronic obstructive pulmonary disease (COPD), and 72 healthy individuals, this device differentiated LC patients from healthy ones with 91.3%, 84.4%, and 94.4% accuracy, sensitivity, and specificity, respectively [146].



**Figure 5.** The schematical representation of an e-nose, consisting of five sensors focusing on the detection of various VOCs.

Dong-Min Kim et al. developed an amperometric sensor based on a dendrimer/AuNP-modified glassy carbon electrode (GSE). AuNPs located in a middle layer between the electrode and dendrimer contributed to the maximum conductivity for the successful detection of two important protein markers, Annexin II and MUC5AC, for the early diagnosis of LC. Thus, this device indirectly provided the LC diagnosis [34]. In addition, CNTs and quantum dots can indirectly contribute to the diagnostic outcome.

Mazzone et al. created an exhaled breath LC biosignature, applying a colorimetric sensor array equipped with chemically reactive colorants. They indicated that the diagnosis accuracy (81.1%) increases when there are evaluated specific histologies considering the clinical risk factors [139]. Furthermore, a modified silicon nanowire field effect transistor (SiNW FET) that showed high accuracy for the detection of LC and discrimination through low- and high-grade cancers was developed [147].

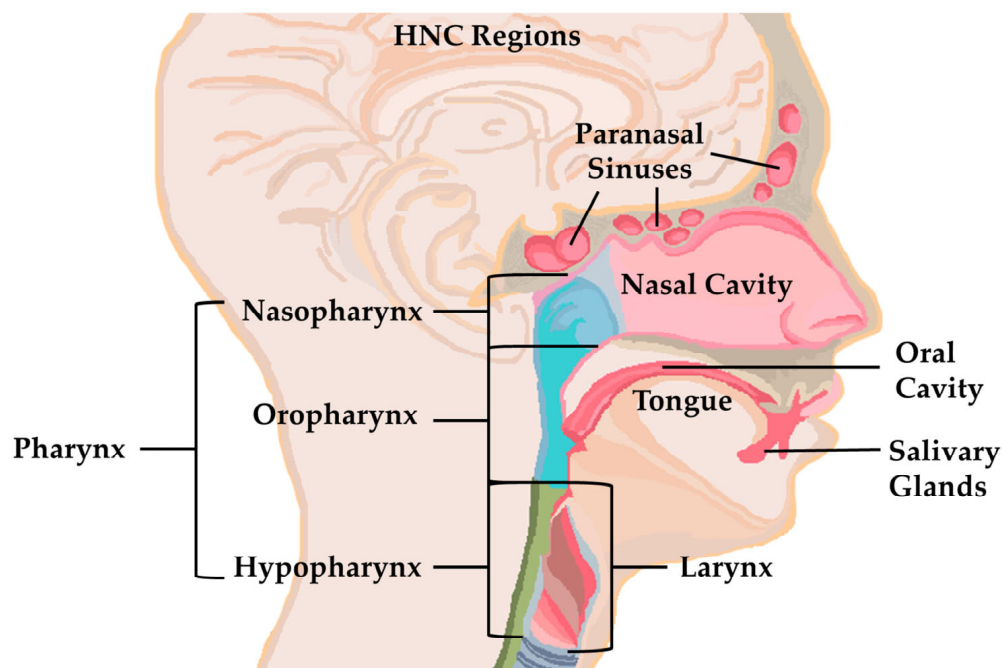
Metalloporphyrins have shown 81% sensitivity and approximately 100% specificity for LC detection through thorough investigation [48,148]. Even though the accuracy, sensitivity, and specificity were high (>85%), the tested sample was small. Thus, further studies should be conducted to verify these findings. Furthermore, metalloporphyrins, porphyrin derivatives, and NaFluo were examined, indicating good sensitivity. NaFluoO was proven to be the most promising of these for commercial use [48,148]. Some characteristic results, obtained by several studies focusing on LC diagnosis through EBA, are shown in Table 7.

**Table 7.** Representative studies focusing on gas sensing for LC diagnosis, using nanosensors.

Nanomaterial	Analytes	Sensor Type	Biological System	Controls	Limit of Detection and Response Time	Validation	Ref
Organic-moleculefunctionalized AuNPs	42 LC biomarkers	chemiresistor	40 individuals	56 individuals	2–10 ppb for Acetaldehyde Response Time: not provided	Gas chromatography–mass spectrometry (GC-MS)	[149]
CNT/hexa-perihexabenzocoronene bilayers	octane decane	chemiresistor	not provided	not provided	15 ppb for octane Response Time: 30 s	GC-MS	[150]
AuNPs	55 VOC biomarkers emitted by NSCLCs (non-small cell LC)	resistance change	cell lines: Calu3, H1650, H4006, H1435, H820, H1975, A549	growth medium without cells in duplicate	10 ppb of trimethylbenzene Response time: 10 s	GC-MS	[151]
Graphene functionalized with Aptameric GFET	Cytokine IL-6	electrochemical	not provided	not provided	2.78 pg/mL Response time: not provided	not provided	[152]
AuNPs	IL-2, IL-4, IL-6, IL-10, IFN- $\gamma$ , and TNF- $\alpha$	Localized Surface Plasmon Resonance	not provided	not provided	11.43 (TNF- $\alpha$ ), 6.46 (IFN- $\gamma$ ), 20.56 (IL-2), 4.60 (IL-4), 11.29 (IL-6), 10.97 pg/mL (IL-10)	ELISA	[153]

### 3.2.3. Nanobiosensors for Use in Head and Neck Cancer Diagnosis

Head and Neck cancer (HNC) is the eighth most frequent malignancy worldwide. HNC is a frequent cause of mortality. In particular, squamous cell carcinoma comprises more than 90% of all HNCs. It typically arises in the mucosa lining of the oral cavity, oropharynx, nasopharynx, hypopharynx, sinonasal tract, and larynx (Figure 6) [154].

**Figure 6.** Regions of Head and Neck Cancers (HNC).

Due to its complexity and the interference with functions such as breathing, eating and speech, a squamous cell carcinoma diagnosis requires a thorough clinical examination with the addition of Computed Tomography/Magnetic Resonance Imaging (CT/MRI) and biopsies [154]. The probability of detecting tumors of the upper aerodigestive tract through breath analysis is high, since their associated VOCs produced from different metabolic cell pathways, particularly at an early stage, can be detected [155]. According to Gruber et al. various chemical groups are significantly distinguished between head and neck

squamous cell carcinoma (HNSCC) patients and healthy individuals, such as nitriles (e.g., 2-propanenitrile, etc.), alcohols (e.g., ethanol, etc.), and alkanes (e.g., undecane, etc.) [156].

According to Dharmawardana et al., there are effective therapies for mucosal HNSCC at an early-stage with limited morbidity, while a poor prognosis is more common in later-stages [4]. It is almost impossible to diagnose early-stage HNSCC over macroscopic clinical signs until patients experience more severe symptoms, and thus they are not referred to a specialist for further evaluation. For this reason, an innovative breath test was applied in that study and was able to detect HNSCC with 80% sensitivity and 86% specificity. This protocol might assist in the detection of HNSCC, as an additional tool, but further research is needed to improve its diagnostic accuracy for early stages [4].

Leunis et al. distinguished HNSCC patients from those without malignancies, using an e-nose, with 90% sensitivity and 80% specificity [157]. Thus, the e-nose might be a potential diagnostic tool for HNSCC. A polymer-based e-nose (CyranoSE 320) was used by Anzivino et al. in a group of 45 subjects (15 with HNC, 15 with allergic rhinitis, and 15 controls), and was able to discriminate (93.3% sensitivity and 86.6% specificity) the breath samples of patients with HNC from controls and from those with allergic rhinitis [158].

In a feasibility study, Van de Goor et al., using an e-nose (aeoNose), were able to discriminate between 40 patients (20 follow-up HNSCC with no evidence of disease and 20 follow-up patients with confirmed locoregional recurrent HNSCC or second/third primary HNSCC, with a sensitivity of 85% and a specificity of 80%. The diagnostic accuracy of this study shows the possibility of using e-nose nanodevices for diagnosing recurrent or primary HNSCC after treatment, and the authors believe that this approach will assist with standard practice to accurately detect follow-up patients with HNSCC and distinguish them from those without malignant disease [159].

Based on the design of a Nanoscale Artificial Nose (NA-Nose) from Tisch and Haick [154], Hakim et al. [160] used a tailor-made NA-NOSE that was based on an array of cross-reactive gas sensors consisting of spherical gold nanoparticles that can differentiate between different odors, forming an artificial olfactory system. The sensitivity with regard to confounding factors (e.g., age, gender, environment, smoking habits) was minimal [160]. This device was able to distinguish between HNC and healthy controls (30 out of 36 samples), HNC and lung cancer patients (40 out of 42 samples), and LC and healthy controls (40 out of 46 samples) [160]. Even though the results proved to be unambiguous, the authors stated that a larger double-blind study was needed to validate this method of diagnosis [160].

Additionally, in a proof-of-concept study, van Hooren et al. (2016), using an e-nose, were able to differentiate the breath samples of 87 patients (53 with HNSCC and 34 with lung carcinoma) with a sensitivity of 85% and a specificity of 84%. Even though the results were promising, the authors agreed that a larger study group in a blinded study was needed to determine if an e-nose may be used as an additional diagnostic tool in the future [161].

A locoregional recurrence of up to 50% is frequently reported, with most of them appearing within the first 2 years after treatment. After initially diagnosing HNSCC, there is a 20% chance of developing a second primary SSC within 5 years. The diagnosis of locoregional recurrence is challenging, especially when the anatomy and the physiology of the region has been severely altered through oncological treatment. As a result, the accuracy of endoscopic procedures and biopsies is negatively influenced. Thus, the improvement of diagnostic methods for patients previously treated with HNSCC, second primary HNSCC, or suspected recurrence is of the uttermost importance [159].

Thus, EBA seems to be efficient in HNC diagnosis, and is expected to be optimized in the near future in order for it to be used as an additional diagnostic tool.

### 3.3. Nanobiosensors for the Diagnosis of Neurodegenerative Diseases

The significant progress in biomedicine inevitably leads to the increased lifespan of the human population, and this fact results in the augmented prevalence of neurodegenerative diseases, such as Alzheimer's disease (AD), Parkinson's disease (PD), and multiple sclerosis (MS) [11,55].



### 3.3.1. Diagnosis of Alzheimer's Disease and Parkinson's Disease

The pathophysiological processes that lead to Alzheimer's disease (AD) typically begin long before any observable symptoms of cognitive impairment appear [63].

AD leads to dementia as a result of neuron damage/destruction, thus resulting in a decline in language, memory, and other cognitive abilities. There is no cure for AD, and thus early disease detection is very important for the management of symptoms and for the improvement of the quality of patient's life [12].

Bach et al. used the Cyranose 320 and ion mobility spectrometry to differentiate AD, PD and healthy controls with a sensitivity of 76.2% and a specificity of 45.8% [48,162]. Cyranose 320 is an e-nose that contains 32 carbon black chemiresistors coated with different polymeric films [48]. By using ion mobility spectrometry (IMS), differences in five VOCs were detected. The researchers used a decision tree approach with four variables to accurately differentiate patients with AD from healthy controls (94% accuracy). The disadvantage of this approach is that the individual chemicals can't distinguish between AD and PD or healthy controls, but only a combination of chemicals in a specific sequence can be used to make a prediction [12].

Tisch et al. demonstrated the feasibility of nanomaterial-based sensors as a diagnostic tool for neurodegenerative diseases. They used an array of 20 organically functionalized SWCNTs and monolayer-capped gold NPs (MCNPs) sensors and gas chromatography (GC)-mass spectroscopy (MS) (GC-MS) and discriminated between AD, PD, and healthy controls with an accuracy of up to 85%. The cross-reactive absorption sites provided by the organic functionalities allowed for the broad detection of breath VOCs. This was due to the varied chemical composition of the gold NPs ligands and organic overlayers on the CNTs, resulting in unique responses. The impact of the organic functionality was greater than any variations between devices, making the breath prints a result of the organic functionality's influence [55].

Lau et al. developed an array of MOS nanosensors mounted on an SnO<sub>2</sub> thin film, coated with Au, Cr or Wo, and they combined these sensors in two different ways. Exhaled breath samples were analyzed using the GC-MS and sensor systems, and the results showed that the chemical components contained in the patient groups were very different from those of healthy people [163]. The combination that had more sensors (8 MOS sensors) showed improved distribution patterns and a better discriminant ability [48].

An array of three electrochemical sensors was utilized in another study to assess the viability of the sensor array idea as a diagnostic biomarker test for AD. This method used sensors to identify three chemical compounds associated with AD. The sensors were made of graphene and a conductive polymer which has a high sensitivity and selectivity, respectively. The sensors work by binding to target molecules and forming imprinted cavities that are specific to the target molecule. To enhance the sensors' performance, a chemical called Prussian blue was added to the graphene. Each sensor was specific to one chemical [62].

Tiele et al. used GC-MS and achieved a 60% sensitivity and 84% specificity in differentiation between mild cognitive impairment (MCI) and AD. In addition, the research detected six VOCs (1-butanol, 2-butanone, acetone, heptanal, 2-propanol and hexanal) that could serve as potential markers for the distinction between MCI and AD [12,48].

The diagnosis of diverse Parkinsonian disorders is associated with a high probability of misdiagnosis and a variety of factors that can cause confusion, especially in the early stages. Nakhleh et al. used both MCNP and SWCNT-based nanosensor arrays in their research. The goal of the study was to accurately distinguish between idiopathic PD (iPD) and other Parkinsonian syndromes (non-iPD) and healthy people [55,164]. The nanosensor array showed a high level of accuracy in distinguishing between iPD and non-iPD parkinsonism, with an accuracy rate of 81%. Furthermore, a second classifier was able to differentiate between non-iPD patients and healthy individuals with 78% accuracy [62]. One advantage of using the nanomaterial-based gas sensor array in this study is its immunity to common confounding factors such as smoking, age, gender, or treatments [164]. This means that the

results obtained from the breath analysis using the nanosensor array are not influenced by other external factors and treatments, leading to more accurate and reliable results. This is a significant benefit in the field of Parkinson's disease diagnosis and research, as it provides a more accurate picture of the disease status of patients.

The breath patterns detected using a combination of nanomaterial-based sensors could serve as a future diagnostic tool for Alzheimer's and Parkinson's diseases. These breath prints are expected to be a cost-effective, fast, and reliable way of diagnosing these diseases [55]. However, these promising findings need to be validated by larger studies, and more participants are needed to determine whether the method is clinically useful [162,164].

### 3.3.2. Multiple Sclerosis Diagnosis

MS is a chronic neurological disease of the central nervous system (CNS) that affects adults aged 20–40 years old [13]. CNS controls our conscious and unconscious functioning; thus, CNS is responsible for the movement and the responses to sensations (e.g., touch, sight, hearing, etc.) through signaling that moves through nerve fibers. Normal nerve fibers are covered with a myelin sheath that accelerates the electrical pulses. Multiple sclerosis is a condition whereby multiple areas throughout the brain and spinal cord are scarred as a result of the attempts of nerve fibers to auto-heal their damage after inflammation [165]. The inflammation damages the insulating myelin sheath cover, and this damage is called de-myelination (Figure 7).

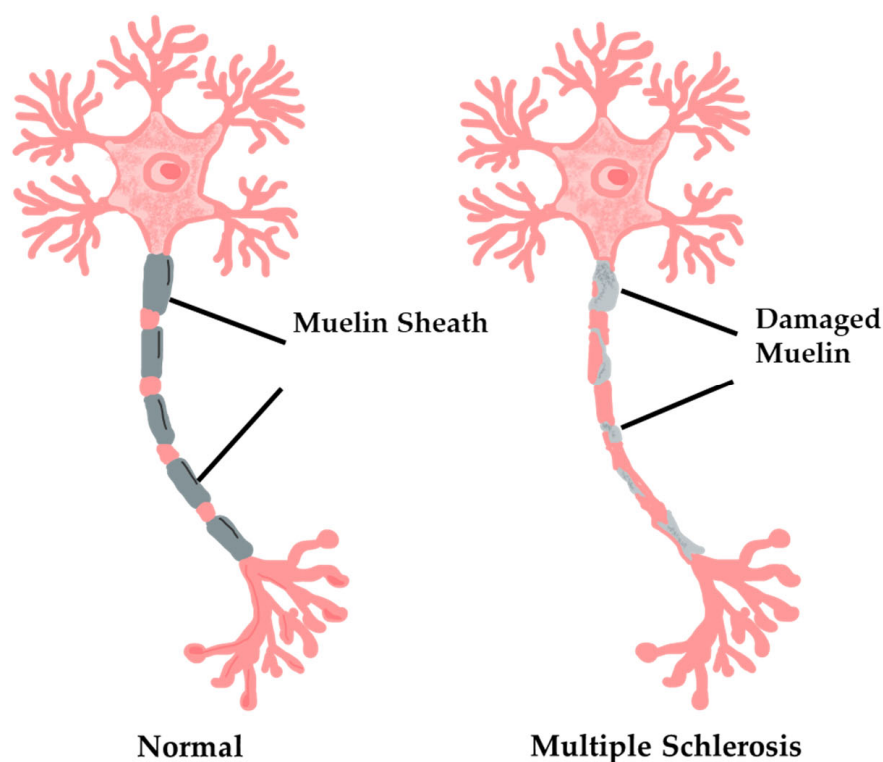


**Figure 7.** Normal and damaged myelin due to multiple sclerosis.

The confirmation of multifocal lesions, the onset of the patient's symptoms, and the supported evidence through MRI and lumbar puncture (which is expensive and quite uncomfortable for the patients) generally lead to an accurate diagnosis [13].

Ionescu et al. used a simple and portable sensing technology and were able to discriminate MS patients' and healthy individuals' exhaled breath samples with 85.3% sensitivity, 70.6% specificity, and 80.4% accuracy [166]. The diagnostic accuracy was comparable to currently available invasive methods [11]. The device had a cross-reactive array of SWCNT bilayers coated with a cap layer of four different polycyclic aromatic hydrocarbons. By

using SWCNT random networks, conductivity variations can be avoided. This sensor array is capable of detecting some VOCs, such as hexanal and 5-methyl-undecane in the breath samples of patients [166]. The aforementioned technology can identify if a patient would respond well to immunotherapy [166] and distinguish between the different subtypes of MS, including remitted MS or relapsed MS, with high accuracy [56].

Ettema et al., using an e-nose device named aeoNose™, distinguished MS patients not using medication from healthy individuals with a sensitivity of 93%, a specificity of 74%, and an overall accuracy of 80% [13]. The aeoNose™ is a commercial MOS-based chemiresistive e-nose [48] that consists of three different, non-specific, micro-hotplate, metal-oxide sensors. When the sensors are exposed to exhaled gas, a redox reaction occurs, resulting in a change in conductivity. By quantifying these changes, the breath print can be obtained [13,58]. Even though these nano-based techniques have high accuracy, no universally recognized breath biomarkers can be used to diagnose MS. In addition, further clinical tests are required [13,56].

Hence, the role of EBA in neurodegenerative disease diagnosis was proven to be significant. This means that the clinical routine should exploit the achievements of nanotechnology for an accurate and fast diagnosis.

#### 4. Conclusions and Future Perspectives

Nanomedicine is a promising scientific field that can dominate in accurate disease diagnosis based on exhaled breath analysis. In biomedicine, the possible application of an individualized therapeutic scheme that is generally able to characterize the diseases at a molecular level has recently become an area of increasing interest. In this framework, the diagnosis of VOC-related diseases exploiting breath analysis by selective and cross-reactive sensors provides an inexpensive, noninvasive, and reliable diagnostic alternative. There remain unknown aspects in this scientific field, but the development of sensors based on biomarkers is a very promising approach. It was already mentioned that some of the desirable characteristics of gas sensors are their fast response, specificity, high sensitivity, compact size, low cost, low power operation at RT, and decreased humidity effect. With regard to the improvement of the absorption of gas molecules, allowing their detection is feasible through the morphology modification of materials. In addition, the selection of a combination of materials that are able to make strong bonds with the analytes might optimize the colorimetric sensors for LC diagnosis, with high specificity and sensitivity, even if the target molecule concentration is low. For this reason, composite, hybrid, and multifunctional materials can be used (e.g., conducting polymers (polypyrrole, polythiophene), molecularly imprinted polymers (in addition to the 3D printing process), in parallel with metal oxides and carbon-based materials. Chemical doping, coating, coupling and morphology modification can improve the sensor response in low concentrations [167]. Advanced data processing and signal amplification as well as data mining are currently applied to the optimized design of very sensitive sensors in low doses of molecules and VOCs [168]. To improve the accuracy and efficiency of medical nano-sensor diagnosis and treatment, artificial intelligence and machine learning algorithms have made significant progress [169]. By training the device signals of the tested sample groups, artificial intelligence, through discriminant factor analysis (DFA), promises a very high accuracy (90–95%) [170].

Nanomaterial-based sensor devices have already been studied for early disease diagnosis and the differential diagnosis of several neurodegenerative diseases, such as AD, PD and MS, diabetes, and also various types of cancer disease. The early-stage and precise diagnosis is of crucial importance for the management of the systematic symptoms and the improvement of the quality of life of patients. Hence, nano-sensors can provide a rapid diagnosis, saving millions of dollars for health systems, while reducing the need for expensive imaging tests using conventional modalities.

It is well established that through breathonomics, such as biomarker discovery, volatolomics (specific VOCs detection), and validation applying conventional diagnostic meth-

ods, the development of rapid tests for disease diagnosis might be achievable, aiding clinicians in identifying some specific infections and diseases. Furthermore, this approach enables earlier medical interventions, and thus leads to a healthier society with reduced mortality rates. There are challenges that still need to be overcome, particularly in the pattern recognition of breath biomarkers that are used in disease diagnosis. In the field of breathonomics and volatolomics, artificial intelligence might contribute by predicting new biomarkers and target molecules and by clarifying the significance of each factor in disease diagnosis [170].

Regarding nanomedicine applications, the design and development of breath sensors with high sensitivity and tunable selectivity is among the desired future perspectives. The “nano” approach can permit approachable, cheaper, smaller, and perhaps wearable devices. Although some optimized breath analysis protocols have been already realized, double-blind studies are needed before these tests can be widely used in the clinical routine.

**Author Contributions:** Conceptualization, N.L. and E.E.; methodology, N.L.; writing—original draft preparation, N.L., T.-F.V., V.P., K.K., N.P., M.-A.G., I.-A.V., S.C., E.A.P., M.G. and E.E.; writing—review and editing, N.L., N.P., E.A.P., M.G. and E.E.; visualization, N.L., T.-F.V., V.P. and K.K.; supervision, N.L. and E.E.; project administration, N.L. All authors have read and agreed to the published version of the manuscript.

**Funding:** This research received no external funding.

**Institutional Review Board Statement:** Not applicable.

**Informed Consent Statement:** Not applicable.

**Data Availability Statement:** Not applicable.

**Acknowledgments:** We would like to thank Anastasios Georgopoulos for his kind support.

**Conflicts of Interest:** The authors declare no conflict of interest.

## References

1. Maxim, L.D.; Niebo, R.; Utell, M.J. Screening tests: A review with examples. *Inhal. Toxicol.* **2014**, *26*, 811–828. [\[CrossRef\]](#) [\[PubMed\]](#)
2. Mokhtar, B.; Kandas, I.; Gamal, M.; Omran, N.; Hassanin, A.H.; Shehata, N. Nano-Enriched Self-Powered Wireless Body Area Network for Sustainable Health Monitoring Services. *Sensors* **2023**, *23*, 2633. [\[CrossRef\]](#) [\[PubMed\]](#)
3. Haselbeck, A.H.; Im, J.; Prifti, K.; Marks, F.; Holm, M.; Zellweger, R.M. Serology as a Tool to Assess Infectious Disease Landscapes and Guide Public Health Policy. *Pathogens* **2022**, *11*, 732. [\[CrossRef\]](#) [\[PubMed\]](#)
4. Dharmawardana, N.; Goddard, T.; Woods, C.; Watson, D.I.; Ooi, E.H.; Yazbeck, R. Development of a non-invasive exhaled breath test for the diagnosis of head and neck cancer. *Br. J. Cancer* **2020**, *123*, 1775–1781. [\[CrossRef\]](#)
5. Bhandari, M.P.; Veliks, V.; Stonāns, I.; Padilla, M.; Šuba, O.; Svare, A.; Krupnova, I.; Ivanovs, N.; Bēma, D.; Mitrovics, J.; et al. Breath Sensor Technology for the Use in Mechanical Lung Ventilation Equipment for Monitoring Critically Ill Patients. *Diagnostics* **2022**, *12*, 430. [\[CrossRef\]](#)
6. Das, S.; Pal, S.; Mitra, M. Significance of Exhaled Breath Test in Clinical Diagnosis: A Special Focus on the Detection of Diabetes Mellitus. *J. Med. Biol. Eng.* **2016**, *36*, 605–624. [\[CrossRef\]](#)
7. Belizário, J.E.; Faintuch, J.; Malpartida, M.G. Breath Biopsy and Discovery of Exclusive Volatile Organic Compounds for Diagnosis of Infectious Diseases. *Front. Cell. Infect. Microbiol.* **2021**, *10*, 564194. [\[CrossRef\]](#)
8. Soodaeva, S.; Kubysheva, N.; Klimanov, I.; Nikitina, L.; Bityrshin, I. Features of Oxidative and Nitrosative Metabolism in Lung Diseases. *Oxid. Med. Cell. Longev.* **2019**, *2019*, 1689861. [\[CrossRef\]](#)
9. Mathew, T.L.; Pownraj, P.; Abdulla, S.; Pullithadathil, B. Technologies for Clinical Diagnosis Using Expired Human Breath Analysis. *Diagnostics* **2015**, *5*, 27–60. [\[CrossRef\]](#)
10. Farrugia, G.; Szurszewski, J.H. Carbon Monoxide, Hydrogen Sulfide, and Nitric Oxide as Signaling Molecules in the Gastrointestinal Tract. *Gastroenterology* **2014**, *147*, 303–313. [\[CrossRef\]](#)
11. Broza, Y.Y.; Haick, H. Nanomaterial-based sensors for detection of disease by volatile organic compounds. *Nanomedicine* **2013**, *8*, 785–806. [\[CrossRef\]](#)
12. Tiele, A.; Wicaksono, A.; Daulton, E.; Ifeachor, E.; Eyre, V.; Clarke, S.; Timings, L.; Pearson, S.; Covington, J.A.; Li, X. Breath-based non-invasive diagnosis of Alzheimer’s disease: A pilot study. *J. Breath Res.* **2020**, *14*, 026003. [\[CrossRef\]](#)
13. Ettema, A.R.; Lenders, M.W.P.M.; Vliegen, J.; Slettenaar, A.; Tjepkema-Cloostermans, M.C.; de Vos, C. Detecting multiple sclerosis via breath analysis using an eNose, a pilot study. *J. Breath Res.* **2021**, *15*, 027101. [\[CrossRef\]](#)



14. Rondanelli, M.; Perdoni, F.; Infantino, V.; Faliva, M.A.; Peroni, G.; Iannello, G.; Nichetti, M.; Alalwan, T.; Perna, S.; Cocuzza, C. Volatile Organic Compounds as Biomarkers of Gastrointestinal Diseases and Nutritional Status. *J. Anal. Methods Chem.* **2019**, *2019*, 7247802. [[CrossRef](#)]
15. Beaver, K.; Dantanarayana, A.; Minter, S.D. Materials Approaches for Improving Electrochemical Sensor Performance. *J. Phys. Chem. B* **2021**, *125*, 11820–11834. [[CrossRef](#)]
16. Jeevanandam, J.; Barhoum, A.; Chan, Y.S.; Dufresne, A.; Danquah, M.K. Review on nanoparticles and nanostructured materials: History, sources, toxicity and regulations. *Beilstein J. Nanotechnol.* **2018**, *9*, 1050–1074. [[CrossRef](#)]
17. Nasiri, N.; Clarke, C. Nanostructured Gas Sensors for Medical and Health Applications: Low to High Dimensional Materials. *Biosensors* **2019**, *9*, 43. [[CrossRef](#)]
18. Lagopati, N.; Evangelou, K.; Falaras, P.; Tsilibary, E.-P.C.; Vasileiou, P.V.S.; Havaki, S.; Angelopoulou, A.; Pavlatou, E.A.; Gorgoulis, V.G. Nanomedicine: Photo-activated nanostructured titanium dioxide, as a promising anticancer agent. *Pharmacol. Ther.* **2021**, *222*, 107795. [[CrossRef](#)]
19. Tremi, I.; Havaki, S.; Georgitsopoulou, S.; Lagopati, N.; Georgakilas, V.; Gorgoulis, V.G.; Georgakilas, A.G. A Guide for Using Transmission Electron Microscopy for Studying the Radiosensitizing Effects of Gold Nanoparticles In Vitro. *Nanomaterials* **2021**, *11*, 859. [[CrossRef](#)]
20. Lagopati, N.; Kotsinas, A.; Veroutis, D.; Evangelou, K.; Papaspyropoulos, A.; Arfanis, M.; Falaras, P.; Kitsiou, P.V.; Pateras, I.; Bergonzini, A.; et al. Biological Effect of Silver-Modified Nanostructured Titanium Dioxide in Cancer. *Cancer Genom. Proteom.* **2021**, *18* (Suppl. 3), 425–439. [[CrossRef](#)]
21. Kalidoss, R.; Kothalam, R.; Manikandan, A.; Jaganathan, S.K.; Khan, A.; Asiri, A.M. Socio-economic demands and challenges for non-invasive disease diagnosis through a portable breathalyzer by the incorporation of 2D nanosheets and SMO nanocomposites. *RSC Adv.* **2021**, *11*, 21216–21234. [[CrossRef](#)] [[PubMed](#)]
22. Munawar, A.; Ong, Y.; Schirhagl, R.; Tahir, M.A.; Khan, W.S.; Bajwa, S.Z. Nanosensors for diagnosis with optical, electric and mechanical transducers. *RSC Adv.* **2019**, *9*, 6793–6803. [[CrossRef](#)] [[PubMed](#)]
23. Lun, D.; Xu, K. Recent Progress in Gas Sensor Based on Nanomaterials. *Micromachines* **2022**, *13*, 919. [[CrossRef](#)] [[PubMed](#)]
24. Qiao, X.; Su, B.; Liu, C.; Song, Q.; Luo, D.; Mo, G.; Wang, T. Selective Surface Enhanced Raman Scattering for Quantitative Detection of Lung Cancer Biomarkers in Superparticle@MOF Structure. *Adv. Mater.* **2018**, *30*, 1702275. [[CrossRef](#)] [[PubMed](#)]
25. Yang, S.; Dai, X.; Stogin, B.B.; Wong, T.-S. Ultrasensitive surface-enhanced Raman scattering detection in common fluids. *Proc. Natl. Acad. Sci. USA* **2015**, *113*, 268–273. [[CrossRef](#)]
26. Pilot, R.; Signorini, R.; Durante, C.; Orian, L.; Bhamidipati, M.; Fabris, L. A Review on Surface-Enhanced Raman Scattering. *Biosensors* **2019**, *9*, 57. [[CrossRef](#)]
27. Fuchs, P.; Loeseken, C.; Schubert, J.K.; Miekisch, W. Breath gas aldehydes as biomarkers of lung cancer. *Int. J. Cancer* **2010**, *126*, 2663–2670. [[CrossRef](#)]
28. Zhang, Z.; Yu, W.; Wang, J.; Luo, D.; Qiao, X.; Qin, X.; Wang, T. Ultrasensitive Surface-Enhanced Raman Scattering Sensor of Gaseous Aldehydes as Biomarkers of Lung Cancer on Dendritic Ag Nanocrystals. *Anal. Chem.* **2017**, *89*, 1416–1420. [[CrossRef](#)]
29. Karakouz, T.; Vaskevich, A.; Rubinstein, I. Polymer-Coated Gold Island Films as Localized Plasmon Transducers for Gas Sensing. *J. Phys. Chem. B* **2008**, *112*, 14530–14538. [[CrossRef](#)]
30. Wang, X.-M.; Li, X.; Liu, W.-H.; Han, C.-Y.; Wang, X.-L. Gas Sensor Based on Surface Enhanced Raman Scattering. *Materials* **2021**, *14*, 388. [[CrossRef](#)]
31. Sun, J.; Lu, Y.; He, L.; Pang, J.; Yang, F.; Liu, Y. Colorimetric sensor array based on gold nanoparticles: Design principles and recent advances. *TRAC Trends Anal. Chem.* **2020**, *122*, 115754. [[CrossRef](#)]
32. Huo, D.; Xu, Y.; Hou, C.; Yang, M.; Fa, H. A novel optical chemical sensor based AuNR-MTPP and dyes for lung cancer biomarkers in exhaled breath identification. *Sens. Actuators B Chem.* **2014**, *199*, 446–456. [[CrossRef](#)]
33. Zhong, X.; Li, D.; Du, W.; Yan, M.; Wang, Y.; Huo, D.; Hou, C. Rapid recognition of volatile organic compounds with colorimetric sensor arrays for lung cancer screening. *Anal. Bioanal. Chem.* **2018**, *410*, 3671–3681. [[CrossRef](#)]
34. Zhang, Y.; Gao, G.; Liu, H.; Fu, H.; Fan, J.; Wang, K.; Chen, Y.; Li, B.; Zhang, C.; Zhi, X.; et al. Identification of Volatile Biomarkers of Gastric Cancer Cells and Ultrasensitive Electrochemical Detection based on Sensing Interface of Au-Ag Alloy coated MWCNTs. *Theranostics* **2014**, *4*, 154–162. [[CrossRef](#)]
35. Obermeier, J.; Trefz, P.; Wex, K.; Sabel, B.; Schubert, J.; Miekisch, W. Electrochemical sensor system for breath analysis of aldehydes, CO and NO. *J. Breath Res.* **2015**, *9*, 016008. [[CrossRef](#)]
36. Homayoonnia, S.; Zeinali, S. Design and fabrication of capacitive nanosensor based on MOF nanoparticles as sensing layer for VOCs detection. *Sens. Actuators B Chem.* **2016**, *237*, 776–786. [[CrossRef](#)]
37. Yang, X.; Chi, H.; Tian, Y.; Li, T.; Wang, Y. Research Progress of Graphene and Its Derivatives towards Exhaled Breath Analysis. *Biosensors* **2022**, *12*, 48. [[CrossRef](#)]
38. Bag, A.; Lee, N.-E. Recent Advancements in Development of Wearable Gas Sensors. *Adv. Mater. Technol.* **2021**, *6*, 2000883. [[CrossRef](#)]
39. Li, T.; Yin, W.; Gao, S.; Sun, Y.; Xu, P.; Wu, S.; Kong, H.; Yang, G.; Wei, G. The Combination of Two-Dimensional Nanomaterials with Metal Oxide Nanoparticles for Gas Sensors: A Review. *Nanomaterials* **2022**, *12*, 982. [[CrossRef](#)]
40. Wu, Z.; Zhang, H.; Ji, H.; Yuan, Z.; Meng, F. Novel combined waveform temperature modulation method of NiO-In<sub>2</sub>O<sub>3</sub> based gas sensor for measuring and identifying VOC gases. *J. Alloys Compd.* **2022**, *918*, 165510. [[CrossRef](#)]



41. Broza, Y.Y.; Vishinkin, R.; Barash, O.; Nakhleh, M.K.; Haick, H. Synergy between nanomaterials and volatile organic compounds for non-invasive medical evaluation. *Chem. Soc. Rev.* **2018**, *47*, 4781–4859. [\[CrossRef\]](#) [\[PubMed\]](#)
42. Lekha, S.; Suchetha, M. Recent Advancements and Future Prospects on E-Nose Sensors Technology and Machine Learning Approaches for Non-Invasive Diabetes Diagnosis: A Review. *IEEE Rev. Biomed. Eng.* **2021**, *14*, 127–138. [\[CrossRef\]](#) [\[PubMed\]](#)
43. Gao, Z.; Lou, Z.; Chen, S.; Li, L.; Jiang, K.; Fu, Z.; Han, W.; Shen, G. Fiber gas sensor-integrated smart face mask for room-temperature distinguishing of target gases. *Nano Res.* **2018**, *11*, 511–519. [\[CrossRef\]](#)
44. Panes-Ruiz, L.A.; Riemenschneider, L.; Al Chawa, M.M.; Löffler, M.; Rellinghaus, B.; Tetzlaff, R.; Bezugly, V.; Ibarlucea, B.; Cuniberti, G. Selective and self-validating breath-level detection of hydrogen sulfide in humid air by gold nanoparticle-functionalized nanotube arrays. *Nano Res.* **2021**, *15*, 2512–2521. [\[CrossRef\]](#) [\[PubMed\]](#)
45. Haick, H. Chemical sensors based on molecularly modified metallic nanoparticles. *J. Phys. D Appl. Phys.* **2007**, *40*, 7173–7186. [\[CrossRef\]](#)
46. Kabir, E.; Raza, N.; Kumar, V.; Singh, J.; Tsang, Y.F.; Lim, D.K.; Szulejko, J.E.; Kim, K.-H. Recent Advances in Nanomaterial-Based Human Breath Analytical Technology for Clinical Diagnosis and the Way Forward. *Chem* **2019**, *5*, 3020–3057. [\[CrossRef\]](#)
47. Behera, B.; Joshi, R.; Vishnu, G.K.A.; Bhalerao, S.; Pandya, H.J. Electronic nose: A non-invasive technology for breath analysis of diabetes and lung cancer patients. *J. Breath Res.* **2019**, *13*, 024001. [\[CrossRef\]](#)
48. Kaloumenou, M.; Skotadis, E.; Lagopati, N.; Efstathiopoulos, E.; Tsoukalas, D. Breath Analysis: A Promising Tool for Disease Diagnosis—The Role of Sensors. *Sensors* **2022**, *22*, 1238. [\[CrossRef\]](#)
49. Kim, I.-D.; Choi, S.-J.; Kim, S.-J.; Jang, J.-S. Exhaled Breath Sensors. In *Smart Sensors for Health and Environment Monitoring*; Kyung, C.M., Ed.; Springer: Dordrecht, The Netherlands, 2015; pp. 19–49. [\[CrossRef\]](#)
50. Ahmed, W.M.; Steenwelle, R.J.A.; Knobel, H.H.; Davie, A.; Steijvers, R.; Verhoeckx, F.; Goodacre, R.; Fowler, S.J.; Rijnders, A.J.H.M.; Nijssen, T.M.; et al. Development of a sensor device with polymer-coated piezoelectric micro-cantilevers for detection of volatile organic compounds. *Meas. Sci. Technol.* **2019**, *31*, 035103. [\[CrossRef\]](#)
51. Rocco, G.; Pennazza, G.; Santonico, M.; Longo, F.; Rocco, R.; Crucitti, P.; Incalzi, R.A. Breathprinting and Early Diagnosis of Lung Cancer. *J. Thorac. Oncol.* **2018**, *13*, 883–894. [\[CrossRef\]](#)
52. Konvalina, G.; Haick, H. Sensors for Breath Testing: From Nanomaterials to Comprehensive Disease Detection. *Acc. Chem. Res.* **2014**, *47*, 66–76. [\[CrossRef\]](#)
53. Julian, T.; Hidayat, S.N.; Rianjanu, A.; Dharmawan, A.B.; Wasisto, H.S.; Triyana, K. Intelligent mobile electronic nose system comprising a hybrid polymer-functionalized quartz crystal microbalance sensor array. *ACS Omega* **2020**, *5*, 29492–29503. [\[CrossRef\]](#)
54. Rianjanu, A.; Fauzi, F.; Triyana, K.; Wasisto, H.S. Electrospun nanofibers for quartz crystal microbalance gas sensors: A review. *ACS Appl. Nano Mater.* **2021**, *4*, 9957–9975. [\[CrossRef\]](#)
55. Tisch, U.; Schlesinger, I.; Ionescu, R.; Nassar, M.; Axelrod, N.; Robertman, D.; Tessler, Y.; Azar, F.; Marmur, A.; Aharon-Peretz, J.; et al. Detection of Alzheimer's and Parkinson's disease from exhaled breath using nanomaterial-based sensors. *Nanomedicine* **2013**, *8*, 43–56. [\[CrossRef\]](#)
56. Zhang, Q.; Dai, X.; Zhang, H.; Zeng, Y.; Luo, K.; Li, W. Recent advances in development of nanomedicines for multiple sclerosis diagnosis. *Biomed. Mater.* **2021**, *16*, 024101. [\[CrossRef\]](#)
57. De Vries, R.; Brinkman, P.; Van Der Schee, M.P.; Fens, N.; Dijkers, E.; Bootsma, S.; De Jongh, F.H.C.; Sterk, P.J. Integration of electronic nose technology with spirometry: Validation of a new approach for exhaled breath analysis. *J. Breath Res.* **2015**, *9*, 046001. [\[CrossRef\]](#)
58. Krauss, E.; Haberer, J.; Barreto, G.; Degen, M.; Seeger, W.; Guenther, A. Recognition of breathprints of lung cancer and chronic obstructive pulmonary disease using the Aeonose<sup>®</sup> electronic nose. *J. Breath Res.* **2020**, *14*, 046004. [\[CrossRef\]](#)
59. Wang, X.R.; Lizier, J.T.; Berna, A.Z.; Bravo, F.G.; Trowell, S.C. Human breath-print identification by E-nose, using information-theoretic feature selection prior to classification. *Sens. Actuators B Chem.* **2015**, *217*, 165–174. [\[CrossRef\]](#)
60. Konvalina, G.; Haick, H. Effect of Humidity on Nanoparticle-Based Chemiresistors: A Comparison between Synthetic and Real-World Samples. *ACS Appl. Mater. Interfaces* **2012**, *4*, 317–325. [\[CrossRef\]](#)
61. Velumani, M.; Prasanth, A.; Narasimman, S.; Chandrasekhar, A.; Sampson, A.; Meher, S.R.; Rajalingam, S.; Rufus, E.; Alex, Z.C. Nanomaterial-Based Sensors for Exhaled Breath Analysis: A Review. *Coatings* **2022**, *12*, 1989. [\[CrossRef\]](#)
62. Nakhleh, M.K.; Broza, Y.Y.; Haick, H. Monolayer-capped gold nanoparticles for disease detection from breath. *Nanomedicine* **2014**, *9*, 1991–2002. [\[CrossRef\]](#) [\[PubMed\]](#)
63. Emam, S.; Nasrollahpour, M.; Colarusso, B.; Cai, X.; Grant, S.; Kulkarni, P.; Ekenseair, A.; Gharagouzloo, C.; Ferris, C.F.; Sun, N. Detection of presymptomatic Alzheimer's disease through breath biomarkers. *Alzheimers Dement* **2020**, *12*, e12088. [\[CrossRef\]](#)
64. American Diabetes Association. Classification and Diagnosis of Diabetes: Standards of Medical Care in Diabetes—2018. *Diabetes Care* **2018**, *41* (Suppl. 1), S13–S27. [\[CrossRef\]](#) [\[PubMed\]](#)
65. Szunerits, S.; Melinte, S.; Barras, A.; Pagneux, Q.; Voronova, A.; Abderrahmani, A.; Boukherroub, R. The impact of chemical engineering and technological advances on managing diabetes: Present and future concepts. *Chem. Soc. Rev.* **2021**, *50*, 2102–2146. [\[CrossRef\]](#)
66. Debele, T.A.; Park, Y. Application of Nanoparticles: Diagnosis, Therapeutics, and Delivery of Insulin/Anti-Diabetic Drugs to Enhance the Therapeutic Efficacy of Diabetes Mellitus. *Life* **2022**, *12*, 2078. [\[CrossRef\]](#)
67. Repaske, D.R. Medication-induced diabetes mellitus. *Pediatr. Diabetes* **2016**, *17*, 392–397. [\[CrossRef\]](#)

68. American Diabetes Association Diagnosis and Classification of Diabetes Mellitus. *Diabetes Care* **2009**, *32*, S62–S67. [\[CrossRef\]](#)
69. American Diabetes Association. 2. Classification and Diagnosis of Diabetes: Standards of Medical Care in Diabetes—2020. *Diabetes Care* **2020**, *43* (Suppl. S1), S14–S31. [\[CrossRef\]](#)
70. Wu, Y.; Ding, Y.; Tanaka, Y.; Zhang, W. Risk Factors Contributing to Type 2 Diabetes and Recent Advances in the Treatment and Prevention. *Int. J. Med. Sci.* **2014**, *11*, 1185–1200. [\[CrossRef\]](#)
71. Marín-Peñalver, J.J.; Martín-Timón, I.; Sevillano-Collantes, C.; Del Cañizo-Gómez, F.J. Update on the treatment of type 2 diabetes mellitus. *World J. Diabetes* **2016**, *7*, 354–395. [\[CrossRef\]](#)
72. Pfeiffer, A.F.; Klein, H.H. The Treatment of Type 2 Diabetes. *Dtsch. Ärzteblatt Int.* **2014**, *111*, 69–82. [\[CrossRef\]](#)
73. Dixit, K.; Fardindoost, S.; Ravishankara, A.; Tasnim, N.; Hoorfar, M. Exhaled Breath Analysis for Diabetes Diagnosis and Monitoring: Relevance, Challenges and Possibilities. *Biosensors* **2021**, *11*, 476. [\[CrossRef\]](#)
74. Fernandez-Morera, J.L.; Rodriguez-Rodero, S.; Menéndez-Torre, E.; Fraga, M.F. The Possible Role of Epigenetics in Gestational Diabetes: Cause, Consequence, or Both. *Obstet. Gynecol. Int.* **2010**, *2010*, 605163. [\[CrossRef\]](#)
75. Lemmerman, L.R.; Das, D.; Higuaita-Castro, N.; Mirmira, R.G.; Gallego-Perez, D. Nanomedicine-Based Strategies for Diabetes: Diagnostics, Monitoring, and Treatment. *Trends Endocrinol. Metab. TEM* **2021**, *31*, 448–458. [\[CrossRef\]](#)
76. Lagopati, N.; Pavlatou, E.A. Nanotechnology in Diabetes Management. *Interv. Obes. Diabetes* **2021**, *5*, 419–424. [\[CrossRef\]](#)
77. Tang, L.; Chang, S.J.; Chen, C.-J.; Liu, J.-T. Non-Invasive Blood Glucose Monitoring Technology: A Review. *Sensors* **2020**, *20*, 6925. [\[CrossRef\]](#)
78. Rydosz, A. Chapter 28—Nanosensors for exhaled breath monitoring as a possible tool for noninvasive diabetes detection. In *Nanosensors for Smart Cities*; Kumar Singh, P., Ed.; Elsevier: Amsterdam, The Netherlands, 2020; pp. 467–481. [\[CrossRef\]](#)
79. Saasa, V.; Malwela, T.; Beukes, M.; Mokgotho, M.; Liu, C.-P.; Mwakikunga, B. Sensing Technologies for Detection of Acetone in Human Breath for Diabetes Diagnosis and Monitoring. *Diagnostics* **2018**, *8*, 12. [\[CrossRef\]](#)
80. Rahman, M.S.; Hossain, K.S.; Das, S.; Kundu, S.; Adegoke, E.O.; Rahman, A.; Hannan, A.; Uddin, J.; Pang, M.-G. Role of Insulin in Health and Disease: An Update. *Int. J. Mol. Sci.* **2021**, *22*, 6403. [\[CrossRef\]](#)
81. O'Brien, P.J.; Siraki, A.G.; Shangari, N. Aldehyde sources, metabolism, molecular toxicity mechanisms, and possible effects on human health. *Crit. Rev. Toxicol.* **2005**, *35*, 609–662. [\[CrossRef\]](#)
82. Vander Jagt, D.L. Methylglyoxal, diabetes mellitus and diabetic complications. *Drug Metab. Pharmacokinet.* **2008**, *23*, 93–124. [\[CrossRef\]](#)
83. Trefz, P.; Schmidt, S.C.; Sukul, P.; Schubert, J.K.; Miekisch, W.; Fischer, D.-C. Non-Invasive Assessment of Metabolic Adaptation in Paediatric Patients Suffering from Type 1 Diabetes Mellitus. *J. Clin. Med.* **2019**, *8*, 1797. [\[CrossRef\]](#) [\[PubMed\]](#)
84. Sharma, A.; Kumar, R.; Varadwaj, P. Smelling the Disease: Diagnostic Potential of Breath Analysis. *Mol. Diagn. Ther.* **2023**, *27*, 321–347. [\[CrossRef\]](#) [\[PubMed\]](#)
85. Moon, H.G.; Jung, Y.; Jun, D.; Park, J.H.; Chang, Y.W.; Park, H.-H.; Kang, C.-Y.; Kim, C.; Kaner, R.B. Hollow Pt-Functionalized SnO<sub>2</sub> Hemipill Network Formation Using a Bacterial Skeleton for the Noninvasive Diagnosis of Diabetes. *ACS Sens.* **2018**, *3*, 661–669. [\[CrossRef\]](#)
86. Jiang, Z.; Yin, M.; Wang, C. Facile synthesis of Ca<sup>2+</sup> / Au co-doped SnO<sub>2</sub> nanofibers and their application in acetone sensor. *Mater. Lett.* **2017**, *194*, 209–212. [\[CrossRef\]](#)
87. Shaikh, F.I.; Chikhale, L.P.; Mulla, I.S.; Suryavanshi, S.S. Synthesis, characterization and enhanced acetone sensing performance of Pd loaded Sm doped SnO<sub>2</sub> nanoparticles. *Ceram. Int.* **2017**, *43*, 10307–10315. [\[CrossRef\]](#)
88. Salehi, S.; Nikan, E.; Khodadadi, A.A.; Mortazavi, Y. Highly sensitive carbon nanotubes–SnO<sub>2</sub> nanocomposite sensor for acetone detection in diabetes mellitus breath. *Sens. Actuators B Chem.* **2014**, *205*, 261–267. [\[CrossRef\]](#)
89. Choi, S.-J.; Jang, B.-H.; Lee, S.-J.; Min, B.K.; Rothschild, A.; Kim, I.-D. Selective detection of acetone and hydrogen sulfide for the diagnosis of diabetes and halitosis using SnO(2) nanofibers functionalized with reduced graphene oxide nanosheets. *ACS Appl. Mater. Interfaces* **2014**, *6*, 2588–2597. [\[CrossRef\]](#)
90. Hu, J.; Yang, J.; Wang, W.; Xue, Y.; Sun, Y.; Li, P.; Lian, K.; Zhang, W.; Chen, L.; Shi, J.; et al. Synthesis and gas sensing properties of NiO/SnO<sub>2</sub> hierarchical structures toward ppb-level acetone detection. *Mater. Res. Bull.* **2018**, *102*, 294–303. [\[CrossRef\]](#)
91. Li, G.; Cheng, Z.; Xiang, Q.; Yan, L.; Wang, X.; Xu, J. Bimetal PdAu decorated SnO<sub>2</sub> nanosheets based gas sensor with temperature-dependent dual selectivity for detecting formaldehyde and acetone. *Sens. Actuators B Chem.* **2019**, *283*, 590–601. [\[CrossRef\]](#)
92. Fioravanti, A.; Marani, P.; Morandi, S.; Lettieri, S.; Mazzocchi, M.; Sacerdoti, M.; Carotta, M.C. Growth Mechanisms of ZnO Micro-Nanomorphologies and Their Role in Enhancing Gas Sensing Properties. *Sensors* **2021**, *21*, 1331. [\[CrossRef\]](#)
93. Alenezi, M.R.; Henley, S.J.; Emerson, N.G.; Silva, S.R.P. From 1D and 2D ZnO nanostructures to 3D hierarchical structures with enhanced gas sensing properties. *Nanoscale* **2014**, *6*, 235–247. [\[CrossRef\]](#)
94. Meng, F.; Hou, N.; Jin, Z.; Sun, B.; Li, W.; Xiao, X.; Wang, C.; Li, M.; Liu, J. Sub-ppb detection of acetone using Au-modified flower-like hierarchical ZnO structures. *Sens. Actuators B Chem.* **2015**, *219*, 209–217. [\[CrossRef\]](#)
95. Xie, Y.; Xing, R.; Li, Q.; Xu, L.; Song, H. Three-dimensional ordered ZnO–CuO inverse opals toward low concentration acetone detection for exhaled breath sensing. *Sens. Actuators B Chem.* **2015**, *211*, 255–262. [\[CrossRef\]](#)
96. Muthukrishnan, K.; Vanaraja, M.; Boomadevi, S.; Kumar Karn, R.; Singh, V.; Singh, P.K.; Pandiyan, K. Studies on acetone sensing characteristics of ZnO thin film prepared by sol–gel dip coating. *J. Alloys Compd.* **2016**, *673*, 138–143. [\[CrossRef\]](#)
97. Li, Y.; Wang, S.; Hao, P.; Tian, J.; Cui, H.; Wang, X. Soft-templated formation of double-shelled ZnO hollow microspheres for acetone gas sensing at low concentration/near room temperature. *Sens. Actuators B Chem.* **2018**, *273*, 751–759. [\[CrossRef\]](#)

98. Koo, A.; Yoo, R.; Woo, S.P.; Lee, H.-S.; Lee, W. Enhanced acetone-sensing properties of Pt-decorated Al-doped ZnO nanoparticles. *Sens. Actuators B Chem.* **2019**, *280*, 109–119. [\[CrossRef\]](#)
99. Yoo, R.; Park, Y.; Jung, H.; Rim, H.J.; Cho, S.; Lee, H.-S.; Lee, W. Acetone-sensing properties of doped ZnO nanoparticles for breath-analyzer applications. *J. Alloys Compd.* **2019**, *803*, 135–144. [\[CrossRef\]](#)
100. Wang, T.; Pysanenko, A.; Dryahina, K.; Španěl, P.; Smith, D. Analysis of breath, exhaled via the mouth and nose, and the air in the oral cavity. *J. Breath Res.* **2008**, *2*, 037013. [\[CrossRef\]](#)
101. Xiao, T.; Wang, X.-Y.; Zhao, Z.-H.; Li, L.; Zhang, L.; Yao, H.-C.; Wang, J.-S.; Li, Z.-J. Highly sensitive and selective acetone sensor based on C-doped WO<sub>3</sub> for potential diagnosis of diabetes mellitus. *Sens. Actuators B Chem.* **2014**, *199*, 210–219. [\[CrossRef\]](#)
102. Kaur, J.; Anand, K.; Kaur, A.; Singh, R.C. Sensitive and selective acetone sensor based on Gd doped WO<sub>3</sub>/reduced graphene oxide nanocomposite. *Sens. Actuators B Chem.* **2018**, *258*, 1022–1035. [\[CrossRef\]](#)
103. Lu, J.; Xu, C.; Cheng, L.; Jia, N.; Huang, J.; Li, C. Acetone sensor based on WO<sub>3</sub> nanocrystallines with oxygen defects for low concentration detection. *Mater. Sci. Semicond. Process.* **2019**, *101*, 214–222. [\[CrossRef\]](#)
104. Deng, L.; Bao, L.; Xu, J.; Wang, D.; Wang, X. Highly sensitive acetone gas sensor based on ultra-low content bimetallic PtCu modified WO<sub>3</sub>-H<sub>2</sub>O hollow sphere. *Chin. Chem. Lett.* **2020**, *31*, 2041–2044. [\[CrossRef\]](#)
105. Zhang, X.; Dong, B.; Liu, W.; Zhou, X.; Liu, M.; Sun, X.; Lv, J.; Zhang, L.; Xu, W.; Bai, X.; et al. Highly sensitive and selective acetone sensor based on three-dimensional ordered WO<sub>3</sub>/Au nanocomposite with enhanced performance. *Sens. Actuators B Chem.* **2020**, *320*, 128405. [\[CrossRef\]](#)
106. Hu, J.; Xiong, X.; Guan, W.; Long, H. Designed construction of PdO@WO<sub>3</sub> core-shell architecture as a high-performance acetone sensor. *J. Environ. Chem. Eng.* **2021**, *9*, 106852. [\[CrossRef\]](#)
107. Wang, Q.; Wu, H.; Wang, Y.; Li, J.; Yang, Y.; Cheng, X.; Luo, Y.; An, B.; Pan, X.; Xie, E. Ex-situ XPS analysis of yolk-shell Sb<sub>2</sub>O<sub>3</sub>/WO<sub>3</sub> for ultra-fast acetone resistive sensor. *J. Hazard. Mater.* **2021**, *412*, 125175. [\[CrossRef\]](#)
108. Choi, H.J.; Chung, J.-H.; Yoon, J.-W.; Lee, J.-H. Highly selective, sensitive, and rapidly responding acetone sensor using ferroelectric  $\epsilon$ -WO<sub>3</sub> spheres doped with Nb for monitoring ketogenic diet efficiency. *Sens. Actuators B Chem.* **2021**, *338*, 129823. [\[CrossRef\]](#)
109. Chang, X.; Xu, S.; Liu, S.; Wang, N.; Sun, S.; Zhu, X.; Li, J.; Ola, O.; Zhu, Y. Highly sensitive acetone sensor based on WO<sub>3</sub> nanosheets derived from WS<sub>2</sub> nanoparticles with inorganic fullerene-like structures. *Sens. Actuators B Chem.* **2021**, *343*, 130135. [\[CrossRef\]](#)
110. Bhise, G.D.; Karpe, S.B.; More, P.; Adhyapak, P.V. Optical fibre based acetone sensor using Pd modified WO<sub>3</sub> nanostructures. *Opt. Laser Technol.* **2022**, *156*, 108566. [\[CrossRef\]](#)
111. Cui, Y.-P.; Shang, Y.-R.; Shi, R.-X.; Che, Q.-D.; Wang, J.-P. Pt-decorated NiWO<sub>4</sub>/WO<sub>3</sub> heterostructure nanotubes for highly selective sensing of acetone. *Trans. Nonferrous Met. Soc. China* **2022**, *32*, 1981–1993. [\[CrossRef\]](#)
112. Kodam, P.M.; Ghadage, P.A.; Nadargi, D.Y.; Shinde, K.; Mulla, I.S.; Park, J.; Suryavanshi, S.S. Ru, Pd doped WO<sub>3</sub> nanomaterials: A synergistic effect of noble metals to enhance the acetone response properties. *Ceram. Int.* **2022**, *48*, 17923–17933. [\[CrossRef\]](#)
113. Sen, S.; Maity, S.; Kundu, S. Fabrication of Fe doped reduced graphene oxide (rGO) decorated WO<sub>3</sub> based low temperature ppm level acetone sensor: Unveiling sensing mechanism by impedance spectroscopy. *Sens. Actuators B Chem.* **2022**, *361*, 131706. [\[CrossRef\]](#)
114. Wang, Q.; Cheng, X.; Wang, Y.; Yang, Y.; Su, Q.; Li, J.; An, B.; Luo, Y.; Wu, Z.; Xie, E. Sea urchins-like WO<sub>3</sub> as a material for resistive acetone gas sensors. *Sens. Actuators B Chem.* **2022**, *355*, 131262. [\[CrossRef\]](#)
115. Zhang, J.; Shao, T.; Dong, J.; Li, G.; Liu, J.; Liu, Y.; Yang, R.; Gao, J.; Li, L.; Jia, Y.; et al. Construction of mesoporous WO<sub>3</sub> nanofibers functionalized with nanoscale PtO catalysts for enhanced acetone sensing properties. *J. Alloys Compd.* **2023**, *933*, 167703. [\[CrossRef\]](#)
116. Shar, A.H.; Lakhan, M.N.; Alali, K.T.; Liu, J.; Ahmed, M.; Shah, A.H.; Wang, J. Facile synthesis of reduced graphene oxide encapsulated selenium nanoparticles prepared by hydrothermal method for acetone gas sensors. *Chem. Phys. Lett.* **2020**, *755*, 137797. [\[CrossRef\]](#)
117. Rathinavel, S.; Balaji, G.; Vadivel, S. High performance ethanol and acetone gas sensing behavior of FeCo<sub>2</sub>O<sub>4</sub>/graphene hybrid sensors prepared by facile hydrothermal route. *Optik* **2020**, *223*, 165571. [\[CrossRef\]](#)
118. Kumar, R.; Ghosh, R. Selective determination of ammonia, ethanol and acetone by reduced graphene oxide based gas sensors at room temperature. *Sens. Bio-Sens. Res.* **2020**, *28*, 100336. [\[CrossRef\]](#)
119. Jang, A.-R.; Lim, J.E.; Jang, S.; Kang, M.H.; Lee, G.; Chang, H.; Kim, E.; Park, J.K.; Lee, J.-O. Ag<sub>2</sub>S nanoparticles decorated graphene as a selective chemical sensor for acetone working at room temperature. *Appl. Surf. Sci.* **2021**, *562*, 150201. [\[CrossRef\]](#)
120. Jia, X.; Yu, S.; Cheng, C.; Yang, J.; Li, Y.; Wang, S.; Song, H. Ag nanoparticles modified Fe<sub>3</sub>O<sub>4</sub>/reduced graphene oxide and their acetone sensing properties. *Mater. Chem. Phys.* **2022**, *276*, 125378. [\[CrossRef\]](#)
121. Geramilla, M.; Muthukumaravel, C.; Karunakaran, U.; Sairam, T. Gold nanoparticle decorated vertical graphene nanosheets composite/hybrid for acetone sensing at room temperature. *Mater. Sci. Eng. B* **2023**, *288*, 116211. [\[CrossRef\]](#)
122. Kim, S.; Park, S.; Sun, G.-J.; Hyun, S.K.; Kim, K.-K.; Lee, C. Enhanced acetone gas sensing performance of the multiple-networked Fe<sub>2</sub>O<sub>3</sub>-functionalized In<sub>2</sub>O<sub>3</sub> nanowire sensor. *Curr. Appl. Phys.* **2015**, *15*, 947–952. [\[CrossRef\]](#)
123. Karmaoui, M.; Leonardi, S.G.; Latino, M.; Tobaldi, D.M.; Donato, N.; Pullar, R.C.; Seabra, M.P.; Labrincha, J.A.; Neri, G. Pt-decorated In<sub>2</sub>O<sub>3</sub> nanoparticles and their ability as a highly sensitive (<10 ppb) acetone sensor for biomedical applications. *Sens. Actuators B Chem.* **2016**, *230*, 697–705. [\[CrossRef\]](#)



124. Li, F.; Zhang, T.; Gao, X.; Wang, R.; Li, B. Coaxial electrospinning heterojunction SnO<sub>2</sub>/Au-doped In<sub>2</sub>O<sub>3</sub> core-shell nanofibers for acetone gas sensor. *Sens. Actuators B Chem.* **2017**, *252*, 822–830. [\[CrossRef\]](#)
125. Zhang, S.; Song, P.; Wang, Q. Enhanced acetone sensing performance of an  $\alpha$ -Fe<sub>2</sub>O<sub>3</sub>-In<sub>2</sub>O<sub>3</sub> heterostructure nanocomposite sensor. *J. Phys. Chem. Solids* **2018**, *120*, 261–270. [\[CrossRef\]](#)
126. Liu, X.; Zhao, K.; Sun, X.; Duan, X.; Zhang, C.; Xu, X. Electrochemical sensor to environmental pollutant of acetone based on Pd-loaded on mesoporous In<sub>2</sub>O<sub>3</sub> architecture. *Sens. Actuators B Chem.* **2019**, *290*, 217–225. [\[CrossRef\]](#)
127. Liu, W.; Xie, Y.; Chen, T.; Lu, Q.; Rehman, S.U.; Zhu, L. Rationally designed mesoporous In<sub>2</sub>O<sub>3</sub> nanofibers functionalized Pt catalysts for high-performance acetone gas sensors. *Sens. Actuators B Chem.* **2019**, *298*, 126871. [\[CrossRef\]](#)
128. Kohli, N.; Hastir, A.; Kumari, M.; Singh, R.C. Hydrothermally synthesized heterostructures of In<sub>2</sub>O<sub>3</sub>/MWCNT as acetone gas sensor. *Sens. Actuators A Phys.* **2020**, *314*, 112240. [\[CrossRef\]](#)
129. Che, Y.; Feng, G.; Sun, T.; Xiao, J.; Guo, W.; Song, C. Excellent gas-sensitive properties towards acetone of In<sub>2</sub>O<sub>3</sub> nanowires prepared by electrospinning. *Colloids Interface Sci. Commun.* **2021**, *45*, 100508. [\[CrossRef\]](#)
130. Feng, G.; Che, Y.; Wang, S.; Wang, S.; Hu, J.; Xiao, J.; Song, C.; Jiang, L. Sensitivity enhancement of In<sub>2</sub>O<sub>3</sub>/ZrO<sub>2</sub> composite based acetone gas sensor: A promising collaborative approach of ZrO<sub>2</sub> as the heterojunction and dopant for in-situ grown octahedron-like particles. *Sens. Actuators B Chem.* **2022**, *367*, 132087. [\[CrossRef\]](#)
131. Hu, J.; Xiong, X.; Guan, W.; Long, H.; Zhang, L.; Wang, H. Self-templated flower-like WO<sub>3</sub>-In<sub>2</sub>O<sub>3</sub> hollow microspheres for conductometric acetone sensors. *Sens. Actuators B Chem.* **2022**, *361*, 131705. [\[CrossRef\]](#)
132. Das, S.; Mahapatra, P.L.; Mondal, P.P.; Das, T.; Pal, M.; Saha, D. A highly sensitive cobalt chromite thick film based trace acetone sensor with fast response and recovery times for the detection of diabetes from exhaled breath. *Mater. Chem. Phys.* **2021**, *262*, 124291. [\[CrossRef\]](#)
133. Jiang, L.; Lv, S.; Tang, W.; Zhao, L.; Wang, C.; Wang, J.; Wang, T.; Guo, X.; Liu, F.; Wang, C.; et al. YSZ-based acetone sensor using a Cd<sub>2</sub>SnO<sub>4</sub> sensing electrode for exhaled breath detection in medical diagnosis. *Sens. Actuators B Chem.* **2021**, *345*, 130321. [\[CrossRef\]](#)
134. Verma, A.; Yadav, D.; Singh, A.; Gupta, M.; Thapa, K.; Yadav, B. Detection of acetone via exhaling human breath for regular monitoring of diabetes by low-cost sensing device based on perovskite BaSnO<sub>3</sub> nanorods. *Sens. Actuators B Chem.* **2022**, *361*, 131708. [\[CrossRef\]](#)
135. Parmar, S.; Ray, B.; Vishwakarma, S.; Rath, S.; Datar, S. Polymer modified quartz tuning fork (QTF) sensor array for detection of breath as a biomarker for diabetes. *Sens. Actuators B Chem.* **2022**, *358*, 131524. [\[CrossRef\]](#)
136. Zhang, Y.; Jia, Q.-Q.; Ji, H.-M.; Yu, J.-J. Semiconducting Nano-structured SmFeO<sub>3</sub>-based Thin Films Prepared by Novel Sol-Gel Method for Acetone Gas Sensors. *Integr. Ferroelectr.* **2014**, *152*, 29–35. [\[CrossRef\]](#)
137. Knight, S.B.; Phil, A.; Crosbie, P.A.; Balata, H.; Chudziak, J.; Hussell, T.; Dive, C. Progress and prospects of early detection in lung cancer. *Open Biol.* **2017**, *7*, 170070. [\[CrossRef\]](#)
138. Roointan, A.; Mir, T.A.; Wani, S.I.; Rehman, M.U.; Hussain, K.K.; Ahmed, B.; Abraham, S.; Savardashtaki, A.; Gandomani, G.; Gandomani, M.; et al. Early detection of lung cancer biomarkers through biosensor technology: A review. *J. Pharm. Biomed. Anal.* **2019**, *164*, 93–103. [\[CrossRef\]](#)
139. Mazzone, P.J.; Wang, X.-F.; Xu, Y.; Mekhail, T.; Beukemann, M.C.; Na, J.; Kemling, J.W.; Suslick, K.; Sasidhar, M. Exhaled Breath Analysis with a Colorimetric Sensor Array for the Identification and Characterization of Lung Cancer. *J. Thorac. Oncol.* **2012**, *7*, 137–142. [\[CrossRef\]](#)
140. Janfaza, S.; Khorsand, B.; Nikkhah, M.; Zahiri, J. Digging deeper into volatile organic compounds associated with cancer. *Biol. Methods Protoc.* **2019**, *4*, bpz014. [\[CrossRef\]](#)
141. Sutaria, S.R.; Gori, S.S.; Morris, J.D.; Xie, Z.; Fu, X.-A.; Nantz, M.H. Lipid Peroxidation Produces a Diverse Mixture of Saturated and Unsaturated Aldehydes in Exhaled Breath That Can Serve as Biomarkers of Lung Cancer—A Review. *Metabolites* **2022**, *12*, 561. [\[CrossRef\]](#)
142. Luo, Y.; Yang, Y.; Peng, P.; Zhan, J.; Wang, Z.; Zhu, Z.; Zhang, Z.; Liu, L.; Fang, W.; Zhang, L. Cholesterol synthesis disruption combined with a molecule-targeted drug is a promising metabolic therapy for EGFR mutant non-small cell lung cancer. *Transl. Lung Cancer Res.* **2021**, *10*, 128–142. [\[CrossRef\]](#)
143. Mazzone, P.J. Analysis of Volatile Organic Compounds in the Exhaled Breath for the Diagnosis of Lung Cancer. *J. Thorac. Oncol.* **2008**, *3*, 774–780. [\[CrossRef\]](#)
144. Ward, N.P.; DeNicola, G.M. Sulfur metabolism and its contribution to malignancy. *Int. Rev. Cell Mol. Biol.* **2019**, *347*, 39–103. [\[CrossRef\]](#) [\[PubMed\]](#)
145. Leemans, M.; Bauër, P.; Cuzuel, V.; Audureau, E.; Fromantin, I. Volatile Organic Compounds Analysis as a Potential Novel Screening Tool for Breast Cancer: A Systematic Review. *Biomark. Insights* **2022**, *17*, 11772719221100709. [\[CrossRef\]](#) [\[PubMed\]](#)
146. Binson, V.A.; Subramoniam, M.; Mathew, L. Discrimination of COPD and lung cancer from controls through breath analysis using a self-developed e-nose. *J. Breath Res.* **2021**, *15*, 046003. [\[CrossRef\]](#)
147. Shehada, N.; Cancilla, J.C.; Torrecilla, J.S.; Pariente, E.S.; Brönstrup, G.; Christiansen, S.; Johnson, D.W.; Leja, M.; Davies, M.P.A.; Liran, O.; et al. Silicon Nanowire Sensors Enable Diagnosis of Patients via Exhaled Breath. *ACS Nano* **2016**, *10*, 7047–7057. [\[CrossRef\]](#) [\[PubMed\]](#)
148. Zhao, S.; Lei, J.; Huo, D.; Hou, C.; Luo, X.; Wu, H.; Fa, H.; Yang, M. A colorimetric detector for lung cancer related volatile organic compounds based on cross-response mechanism. *Sens. Actuators B Chem.* **2018**, *256*, 543–552. [\[CrossRef\]](#)

149. Peng, G.; Tisch, U.; Adams, O.; Hakim, M.; Shehada, N.; Broza, Y.Y.; Billan, S.; Abdah-Bortnyak, R.; Kuten, A.; Haick, H. Diagnosing lung cancer in exhaled breath using gold nanoparticles. *Nat. Nanotechnol.* **2009**, *4*, 669–673. [\[CrossRef\]](#)
150. Zilberman, Y.; Tisch, U.; Shuster, G.; Pisula, W.; Feng, X.; Müllen, K.; Haick, H. Carbon nanotube/hexa-perihexabenzocoronene bilayers for discrimination between nonpolar volatile organic compounds of cancer and humid atmospheres. *Adv. Mater.* **2010**, *22*, 4317–4320. [\[CrossRef\]](#)
151. Barash, O.; Peled, N.; Hirsch, F.R.; Haick, H. Sniffing the unique “odor print” of non-small-cell lung cancer with gold nanoparticles. *Small* **2009**, *5*, 2618–2624. [\[CrossRef\]](#)
152. Hao, Z.; Pan, Y.; Huang, C.; Wang, Z.; Zhao, X. Sensitive detection of lung cancer biomarkers using an aptameric graphene-based nanosensor with enhanced stability. *Biomed. Microdevices* **2019**, *21*, 65. [\[CrossRef\]](#)
153. Chen, P.; Chung, M.T.; McHugh, W.; Nidetz, R.; Li, Y.; Fu, J.; Cornell, T.T.; Shanley, T.P.; Kurabayashi, K. Multiplex serum cytokine immunoassay using nanoplasmonic biosensor microarrays. *ACS Nano* **2015**, *9*, 4173–4181. [\[CrossRef\]](#) [\[PubMed\]](#)
154. Tisch, U.; Haick, H. Nanomaterials for cross-reactive sensor arrays. *MRS Bull.* **2010**, *35*, 797–803. [\[CrossRef\]](#)
155. Lang, H.P.; Loizeau, F.; Hiou-Feige, A.; Rivals, J.-P.; Romero, P.; Akiyama, T.; Gerber, C.; Meyer, E. Piezoresistive Membrane Surface Stress Sensors for Characterization of Breath Samples of Head and Neck Cancer Patients. *Sensors* **2016**, *16*, 1149. [\[CrossRef\]](#) [\[PubMed\]](#)
156. Gruber, M.L.; Tisch, U.; Jeries, R.; Amal, H.; Hakim, M.; Ronen, O.; Marshak, T.; Zimmerman, D.R.; Israel, O.; Amiga, E.; et al. Analysis of exhaled breath for diagnosing head and neck squamous cell carcinoma: A feasibility study. *Br. J. Cancer* **2014**, *111*, 790–798. [\[CrossRef\]](#) [\[PubMed\]](#)
157. Leunis, N.; Boumans, M.; Kremer, B.; Din, S.; Stobberingh, E.; Kessels, A.G.H.; Kross, K.W. Application of an electronic nose in the diagnosis of head and neck cancer. *Laryngoscope* **2013**, *124*, 1377–1381. [\[CrossRef\]](#)
158. Anzivino, R.; Sciancalepore, P.I.; Dragonieri, S.; Quaranta, V.N.; Petrone, P.; Petrone, D.; Quaranta, N.; Carpagano, G.E. The Role of a Polymer-Based E-Nose in the Detection of Head and Neck Cancer from Exhaled Breath. *Sensors* **2022**, *22*, 6485. [\[CrossRef\]](#)
159. van de Goor, R.M.G.E.; Hardy, J.C.A.; van Hooren, M.R.A.; Kremer, B.; Kross, K.W. Detecting recurrent head and neck cancer using electronic nose technology: A feasibility study. *Head Neck* **2019**, *41*, 2983–2990. [\[CrossRef\]](#)
160. Hakim, M.; Billan, S.; Tisch, U.; Peng, G.; Dvorkind, I.; Marom, O.; Abdah-Bortnyak, R.; Kuten, A.; Haick, H. Diagnosis of head-and-neck cancer from exhaled breath. *Br. J. Cancer* **2011**, *104*, 1649–1655. [\[CrossRef\]](#)
161. Van Hooren, M.R.A.; Leunis, N.; Brandsma, D.S.; Dingemans, A.-M.C.; Kremer, B.; Kross, K.W. Differentiating head and neck carcinoma from lung carcinoma with an electronic nose: A proof of concept study. *Eur. Arch. Otorhinolaryngol.* **2016**, *273*, 3897–3903. [\[CrossRef\]](#)
162. Bach, J.-P.; Gold, M.; Mengel, D.; Hattesohl, A.; Lübke, D.; Schmid, S.; Tackenberg, B.; Rieke, J.; Maddula, S.; Baumbach, J.I.; et al. Measuring Compounds in Exhaled Air to Detect Alzheimer’s Disease and Parkinson’s Disease. *PLoS ONE* **2015**, *10*, e0132227. [\[CrossRef\]](#)
163. Lau, H.-C.; Yu, J.-B.; Lee, H.-W.; Huh, J.-S.; Lim, J.-O. Investigation of Exhaled Breath Samples from Patients with Alzheimer’s Disease Using Gas Chromatography-Mass Spectrometry and an Exhaled Breath Sensor System. *Sensors* **2017**, *17*, 1783. [\[CrossRef\]](#)
164. Nakhleh, M.; Badarny, S.; Winer, R.; Jeries, R.; Finberg, J.; Haick, H. Distinguishing idiopathic Parkinson’s disease from other parkinsonian syndromes by breath test. *Park. Relat. Disord.* **2015**, *21*, 150–153. [\[CrossRef\]](#)
165. Modrak, M.; Talukder, M.A.H.; Gurgenshvili, K.; Noble, M.; Elfar, J.C. Peripheral nerve injury and myelination: Potential therapeutic strategies. *J. Neurosci. Res.* **2020**, *98*, 780–795. [\[CrossRef\]](#)
166. Ionescu, R.; Broza, Y.; Shaltieli, H.; Sadeh, D.; Zilberman, Y.; Feng, X.; Glass-Marmor, L.; Lejbkowitz, I.; Müllen, K.; Miller, A.; et al. Detection of multiple sclerosis from exhaled breath using bilayers of polycyclic aromatic hydro-carbons and single-wall carbon nanotubes. *ACS Chem. Neurosci.* **2011**, *2*, 687–693. [\[CrossRef\]](#)
167. Pathak, A.K.; Swargiary, K.; Kongsawang, N.; Jitpratak, P.; Ajchareeyasoontorn, N.; Udomkittivorakul, J.; Vipavakit, C. Recent Advances in Sensing Materials Targeting Clinical Volatile Organic Compound (VOC) Biomarkers: A Review. *Biosensors* **2023**, *13*, 114. [\[CrossRef\]](#)
168. Purohit, B.; Vernekar, P.R.; Shetti, N.P.; Chandra, P. Biosensor nanoengineering: Design, operation, and implementation for biomolecular analysis. *Sens. Int.* **2020**, *1*, 100040. [\[CrossRef\]](#)
169. Chen, M.; Cui, D.; Haick, H.; Tang, N. Artificial Intelligence-Based Medical Sensors for Healthcare System. *Adv. Sens. Res.* **2023**, *Early View*, 2300009. [\[CrossRef\]](#)
170. Hu, W.; Wu, W.; Jian, Y.; Haick, H.; Zhang, G.; Qian, Y.; Yuan, M.; Yao, M. Volatolomics in healthcare and its advanced detection technology. *Nano Res.* **2022**, *15*, 8185–8213. [\[CrossRef\]](#)

**Disclaimer/Publisher’s Note:** The statements, opinions and data contained in all publications are solely those of the individual author(s) and contributor(s) and not of MDPI and/or the editor(s). MDPI and/or the editor(s) disclaim responsibility for any injury to people or property resulting from any ideas, methods, instructions or products referred to in the content.